The use of a vortex insertion technique to simulate the extratropical transition of Hurricane Michael (2000)

03 August 2006

Abstract

On 19 October 2000, Hurricane Michael merged with an approaching baroclinic trough over the western North Atlantic Ocean south of Nova Scotia. As the hurricane moved over cooler sea surface temperatures (SSTs, less than 25^{o}C) it intensified to category-two intensity on the Saffir-Simpson hurricane scale (maximum sustained wind speeds of 44 m s^{-1} (85 kts)) while tapping energy from the baroclinic environment. The large "hybrid" storm made landfall on the south coast of Newfoundland with maximum sustained winds of 39 m s^{-1} (75 kts) causing moderate damage to coastal communities east of landfall.

Hurricane Michael presented significant challenges to weather forecasters. The fundamental issue was determining which of two cyclones (a newly-formed baroclinic low south of Nova Scotia, or the hurricane) would become the dominant circulation center (during the early stages of the extratropical transition (ET) process). Secondly, it was difficult to predict the intensity of the storm at landfall owing to competing factors: 1) decreasing SSTs conducive to weakening and 2) the approaching upper-level trough, favoring intensification.

Numerical hindcast simulations using the limited-area Mesoscale Compressible Community model (MC2) with synthetic vortex insertion (cyclone bogus) prior to the ET of Hurricane Michael lead to a more realistic evolution of wind and pressure compared to running the model without vortex insertion. Specifically, the mesoscale model correctly simulates the hurricane as the dominant circulation center early in the transition process,

versus the baroclinic low to its north, which was the favored development in the runs not employing vortex insertion. A suite of experiments is conducted to establish the sensitivity of the ET to various initial conditions, lateral driving fields, domain sizes and model parameters. The resulting storm tracks and intensities fall within the range of operational guidance**,** lending support to the possibility of improving numerical forecasts using synthetic vortex insertion prior to ET in such a model.

Introduction

a. Background

Many numerical weather prediction models used to study and predict the movement and intensity of tropical cyclones (TCs) rely on an accurate representation of the storm in the initial conditions. There are various means by which numerical TC models are initialized. Most are initialized with a synthetic hurricane vortex (also known as a "bogus" vortex and referred to as "vortex specification") which is an idealized three-dimensional representation of the real storm in gradient wind balance with a symmetric moist core structure, extending through the troposphere. The synthetic vortex is typically constructed prior to running the primary forecast or research model, then inserted and blended with the ambient meteorological fields, giving improved initial conditions for the model.

Agencies that utilize a synthetic vortex or synthetic observations to initiate numerical hurricane forecast models include the United Kingdom Meteorological Office (UKMO or UKMET), the Geophysical Fluid Dynamics Laboratory (GFDL), and the Tropical Cyclone-Limited Area Prediction System (TC-LAPS) developed at the Australian Bureau of Meteorology Research Centre (BMRC), among others. The UKMET global model is initialized with synthetic tangential surface wind observations located at specific points around the storm center, and at specified vertical levels (Heming and Radford 1998). The synthetic winds are matched as closely as possible to real information on storm intensity, provided by the National Hurricane Center (NHC). A second example is the GFDL

model which has a more sophisticated vortex initialization scheme whereby an axisymmetric version of the primary (GFDL) model is used to build an idealized vortex, run for 60 hours from an initially motionless state (Kurihara et al. 1995). During the vortex generation phase, the wind field of the developing vortex is "nudged" toward a target wind field that is consistent with the real storm. The fully developed vortex is then inserted and blended with the ambient environment, providing the initial atmospheric state for the main model run. The ambient environment and lateral boundary conditions for the limited-area GFDL model are provided by the Global Forecast System (GFS). As a third example, the TC-LAPS prediction system merges synthetic observations from the storm region, with large scale (real) observations to produce coarse and high resolution objective analyses from a four-dimensional data assimilation procedure (Davidson and Weber 2000). The synthetic observations are taken from a three-dimensional synthetic idealized vortex constructed using information on observed storm size, storm motion, and intensity (Davidson et al. 1993). A 24-hour diabatic, dynamical nudging integration using satellite imagery is run with output from the high resolution objective analysis as the initial condition. The output from this integration produces the initial conditions for the main high resolution forecast, which is driven at the lateral boundaries by a comparatively coarse limited area forecast model.

Vortex specification is a suitable approach for initializing numerical hurricane models when the TC is well-developed (at least hurricane strength) in the tropical or subtropical latitudes, and is not experiencing dramatic structural changes owing to environmental influences, such as vertical wind shear. The procedures described above can generally be

applied until the storm moves out of the subtropics, moves over land, weakens over cold water, or undergoes extratropical transition (ET).

Relatively little is known about the affect and appropriateness of employing vortex specification on numerical simulations of ET. Jones et al. (2003) caution that continued implementation of a synthetic vortex (as a TC migrates into the middle latitudes) may delay the onset of ET in the numerical model. Evans et al. (2006) analyzed the impact of vortex specification on the evolution of ET in the context of cyclone phase space analyses developed by Hart (2003). They found that employing vortex insertion improves the numerical forecasts during the early stages of ET, but can degrade the forecast later in the integration. Given this behavior, employing vortex insertion prior to ET may only have utility over short forecast periods (on the order of 24 to 36 hours according to Evans et al. 2006). In a study of eight transitioning TCs in the Atlantic Basin, Hart and Evans (2004) found that storms initialized with a synthetic vortex prior to transition were likely to retain an exaggerated warm core structure after ET was complete, when compared with a model that employed vortex relocation.[1] On the other hand, an initially weakly-represented TC may undergo ET too soon.

Different approaches for initializing the TC in numerical case studies of ET have been applied. For example, McTaggart-Cowan et al. (2001) conducted numerical simulations of the ET of Hurricane Earl in 1998. Their simulations were initialized directly from

[1] Vortex relocation is used in the GFS whereby the forecast of the storm from a previous run of the model is simply relocated to the observed storm position. The relocated vortex is typically weaker but larger than a synthetically-inserted one.

objective analyses (~35 km horizontal resolution) after the storm had weakened from its tropical phase, but before a period of significant reintensification. A synthetic vortex was not necessary in this case since the low pressure area was adequately represented in the analysis. In a numerical study of the heavy rainfall during the ET of Hurricane Floyd in 1999, Colle (2003) initialized simulations using zero-hour Eta model fields (~32 km horizontal resolution). The intensity of Floyd was ~25 hPa too weak in the initial conditions, but this did not appear to have a negative impact on the heavy precipitation during the simulated ET event in that study. Klein et al. (2002) use Navy Operational Global Atmospheric Prediction System 1^{o} lat-lon analyses to initialize numerical simulations of the ET of Typhoon Bart in 1999. The TC in these analyses consists of synthetic vertical profiles of standard meteorological variables, which are based on a simple symmetric Rankine vortex. Numerical simulations of the ET of Hurricane Irene in 1999 (Agusti-Panareda et al. 2004) were initialized from UKMET analyses which also contain synthetic TC observations, as discussed earlier. Representation of the TC using synthetic observations on rather coarse grid domains seems to be sufficient for conducting meaningful simulations and sensitivity studies in these studies.

Numerical sensitivity studies of hurricanes interacting with various idealistic middle latitude trough and environmental wind shear patterns (characteristic of ET) have been investigated by Frank and Ritchie (1999) and by Kimball and Evans (2002) using synthetic TC vortices in the initial conditions, with positive results. In a study by Ritchie and Elsberry (2001), the initial TC vortex for the numerical model is spun up from a quiescent environment to an intensity of a category-three hurricane. This served as the

pre-transition storm vortex that was inserted into various idealistic environmental wind patterns to simulate ET. This approach was successful in reproducing cloud and rainfall patterns of observed storms in similar environments.

More recently, Fogarty et al. (2006) and McTaggart-Cowan et al. (2006) have successfully simulated the landfall of Hurricane Juan in 2003, and the eventual extratropical transition over Eastern Canada, by directly inserting a synthetic hurricane vortex into the large scale analysis fields. These hindcasts were a significant improvement over global numerical forecasts not employing vortex insertion.

b. Case overview

On 17 October 2000 meteorologists at the Meteorological Service of Canada (MSC) and the Canadian Hurricane Centre (CHC) were monitoring the development of Hurricane Michael some 500 km west-southwest of Bermuda. The large-scale atmospheric flow suggested that the hurricane would move northeastward toward eastern Nova Scotia or Newfoundland and would require the issuance of forecast bulletins and warnings by the CHC.

While the CHC began issuing warnings on the storm, the weather research group at the MSC was considering Michael as a candidate storm for a research aircraft mission. Plans to conduct such a flight had been in the works prior to the formation of Michael in order to gather data and gain insight into the structural changes taking place in storms

undergoing ET. On 18 October a mission was arranged by the MSC in partnership with the Canadian National Research Council (NRC) to fly the Convair 580 aircraft (owned and operated by the NRC) into Hurricane Michael southeast of Nova Scotia. A summary of the research mission and the meteorological data that was collected is discussed by Abraham et al. (2004).

Almost six years after the storm we have returned to this case from a numerical modeling standpoint. The primary focus of this work is to simulate the evolution of Hurricane Michael with the Mesoscale Compressible Community (MC2) model (Benoit et al. 1997) to demonstrate how simple insertion of a synthetic TC vortex (consistent with observed location, intensity and size) into the model initial conditions (Davidson et al. 1993) prior to the onset of ET, leads to an improved hindcast of the event. The model is initiated using only observational data (~24 hours prior to landfall) that would have been available in real time, as if being run in forecast mode. Furthermore, we use the model to diagnose structural changes in the storm during ET, compare the results with aircraft data and surface meteorological observations, and test the sensitivity of the transition to various controllable parameters.

The specific operational forecast challenge with extratropically-transitioning Hurricane Michael was determining whether the hurricane, or a new baroclinic (i.e. frontal) cyclone north of the hurricane, would become the dominant storm center as the ET event unfolded. Unfortunately, operational weather forecasters at the CHC did not have much information in terms of high-resolution numerical guidance at the time. The Canadian

Global Environmental Multiscale (GEM) forecast model (the primary weather forecast model in Canada) incorrectly developed the new baroclinic cyclone since the hurricane (which in reality became the dominant storm center early on in the transition) was poorly represented in the initial conditions. Furthermore, the GEM model at the time only had a horizontal resolution of 24 km in its high resolution window, which is insufficient for modeling hurricanes.

The situation is summarized below in a quote from the forecast bulletin issued at 12 UTC 19 October 2000 by the CHC:

"THE NEW BAROCLINIC LOW HAS APPEARED AROUND 05Z AND IS INTENSIFYING RAPIDLY. AT 09Z IT WAS LOCATED BETWEEN BUOY 44142 AND THE NOVA SCOTIA COAST. THE TWO SYSTEMS WILL EVENTUALLY MERGE INTO AN INTENSE MID-LATITUDE LOW. THE PROBLEM REMAINS WHERE THE MERGER WILL TAKE PLACE AND WHICH SYSTEM WILL BECOME DOMINANT."

Late in the morning of 19 October it became apparent to forecasters that the hurricane would remain the dominant circulation center as the lows merged, but there was still considerable uncertainty about how the storm was going to evolve during its approach to Newfoundland. These issues resulted in only a short forecast lead-time for severe conditions in southern Newfoundland. It will become apparent in this paper how the mesoscale modeling approach with synthetic vortex insertion would provide useful guidance if run in a forecast setting for this event.

The remainder of this paper is organized as follows. In section 2 we give a synoptic summary of Hurricane Michael. In section 3 we describe the modeling system with grid configurations and in section 4 results from the control experiments will be given. Results from a series of sensitivity experiments are discussed and compared with operational forecast models in section 5, and a summary of the results with concluding remarks appears in section 6.

2. Synoptic history of Hurricane Michael

Hurricane Michael originally formed from an extratropical low pressure system to the southwest of Bermuda from 12 to 15 October 2000, as described in detail by Davis and Bosart (2003). At 12 UTC 15 October (hereafter we use hour/day UTC, i.e. 12/15) the large cyclonic system had developed organized convection near its center and was declared a subtropical depression by the NHC. A day and a half later at 00/17 it was designated as Tropical Storm Michael and by 18/17 Michael had reached hurricane strength with maximum sustained winds near 33 m s^{-1} (65 kts). A complete storm track with sea surface temperatures (SSTs) valid at 00/19 is shown in Fig. 1 and a time trace plot of the "best track" (BT) (Stewart 2000) data is shown in Fig. 2. The tracking data is a combination of data from Stewart (2000) with minor refinements by Abraham et al. (2004) in the vicinity of Newfoundland.

On 18 October Michael began to accelerate toward the northeast as it moved into the region of stronger environmental winds north of 30^{o}N. These winds caused a spreading-out of high clouds to the north of Michael as shown in Fig. 3a. Michael reached its maximum pre-ET intensity with maximum sustained surface winds of 39 m s^{-1} (75kts) at 00/19 (Fig. 3b). Extratropical transition began around 00/19 based on the cyclone phase space (Hart 2003) trajectory from the Aviation Model (AVN) analyses shown in Fig. 4. Approximately 6 hours after the onset of ET, significant intensification took place at a rate of at least -2 hPa/hr while interacting with a sharpening mid-tropospheric trough (Fig. 3f) and a strong surface baroclinic zone (not shown). Michael was also accelerating very rapidly during this period with maximum forward translational speeds near 30 m s^{-1} over decreasing SSTs (see SSTs in Fig. 1). The storm made landfall at 2230/19 on the south coast of Newfoundland with maximum sustained winds near 39 m s^{-1} (75 kts). At that time, the storm was rapidly loosing tropical characteristics as evidenced in the satellite imagery in Fig. 3 and the cyclone phase space (CPS) in Fig. 4. The NHC had declared Michael as extratropical at 00/20, consistent with the CPS diagram showing the cross-over time from "asymmetric warm core" to "asymmetric cold core". This cross-over delineates the end of ET as defined by Evans and Hart (2003). For additional synoptic information on this event, the reader is referred to Abraham et al. (2004).

The lifecycle of the baroclinic low introduced in the previous section began around 06/19 approximately 200 km south of Cape Sable, Nova Scotia. A subjective (i.e. manually drawn) sea level pressure analysis of the hurricane and this baroclinic low at 12/19 is shown in Fig. 5. The key to identifying a circulation in that region came from a weather

buoy (44142), which showed light southwest winds just south of the estimated center of the low in Fig. 5. The low tracked toward the northeast initially, then toward the east after 12/19. By 18/19 the sea level pressure center of the baroclinic low (indicating the surface circulation) was becoming less distinct while the primary circulation became centered at the location of the hurricane. In section 4 we will discuss the evolution of this low in more detail.

3. Description of the modeling system

a. The mesoscale atmospheric model

The Mesoscale Compressible Community (MC2) model (version 4.9.6) is used to conduct experiments simulating Hurricane Michael using a synthetic TC vortex insertion in the initial conditions. This non-hydrostatic, fully compressible limited area model employs three-dimensional semi-Lagrangian advection and semi-implicit time discretization to solve the primitive Euler equations on terrain-following height coordinates (Gal-Chen and Somerville 1975). Version 4.0 of the Canadian Meteorological Center (CMC) Physics Library is used for the parameterization of physical processes. A kinetic energy closure scheme described by Benoit et al. (1989) is employed in the boundary layer to parameterize turbulent transports. Monin-Obukhov similarity theory (Monin and Obukhov 1954) is used in the atmospheric surface layer to determine the vertical profile of the wind field and sea surface fluxes. Standard bulk

formulations are used to represent turbulent fluxes of momentum, sensible heat and latent heat at the lower boundary. Wind, temperature and humidity used to compute these fluxes are taken from the lowest computational level in the model. The force-restore surface scheme (Benoit et al. 1989) is used in all simulations to predict the surface temperature and moisture budget over land. Deep convective processes are handled with Kain and Fritsch (1990) convective parameterization in the control simulations on the coarser (12 km) grid, but solved explicitly on the fine (3 km) grid, described below. Shallow convective processes are solved explicitly in all the experiments. Stratiform condensation (cloud microphysical) schemes are given by Tremblay et al. (1996) for the 12 km simulations and Kong and Yau (1997) for the 3 km runs. For a general overview of the model see Benoit et al. (1997).

Grid configurations and model integration periods are shown in Fig. 6. The model is piloted (forced at the lateral boundaries) by regional analyses every six hours from the CMC Data Assimilation System archive (Chouinard et al. 1994) on a 28 km (0.25^o) latitude-longitude grid covering eastern North America and the Western Atlantic Ocean (20.0^oN to 70.0^oN and 100.0^oW to 30.0^oW). Integrations of the model are run on three different grids. Two of the grids (one large and one small) have a horizontal resolution of 12 km (0.108^o) while the third has a horizontal resolution of 3 km (0.027^o). The large 12 km latitude-longitude grid extends from 21.3^oN to 64.5^oN and from 88.2^oW to 35.8^oW with 25 computational levels (7 in the atmospheric boundary layer (BL)). The smaller 12 km grid spans from 25.4^oN to 54.6^oN and from 78.2^oW to 45.8^oW with the same number of computational levels. The finest grid at 3 km resolution includes Nova Scotia and

Newfoundland from 36.2°N to 49.7°N and from 65.7°W to 52.2°W with 40 computational levels (12 in the BL). The lowest computational level in the 3 km grid is 40 m. A time step of 120 seconds is used on the 12 km domains and 30 seconds for the 3 km domain.

b. The synthetic storm vortex

The initial atmospheric fields are modified by inserting a synthetic TC vortex constructed prior to running the model[2]. The poorly-analysed hurricane in the original fields is very near the location where we insert the synthetic vortex, so the original low is completely replaced. The vortex is constructed using key observational data from the NHC best track (Stewart 2000) and from NHC operational message archives (available online at: http://www.nhc.noaa.gov/archive/2000/MICHAEL.html). Control parameters for the vortex include: (a) the minimum central sea level pressure, (b) storm center position, (c) size (radius of 15 m s^{-1} surface winds, R_{15}) and (d) the percent of the background flow used for the initial wind field asymmetry. The sea level pressure profile follows that of Fujita (1952) and is defined as a function of radius:

$$p(r) = p_e - dp\left[1 + \left(\frac{r}{R_o}\right)^2\right]^{-\frac{1}{2}} \qquad (1)$$

[2] This synthetic vortex is very similar to the one used in the TC-LAPS (section 1) and is described by Davidson et al. (1993).

where $dp = p_e - p_c$ (p_e is the ambient sea level pressure and p_c is the minimum sea level pressure in the storm). R_o is the *characteristic* radius (smaller R_o yields a larger radial pressure gradient). For example, for a given dp, if R_{15} is decreased to give a compact storm, then R_o will also decrease. The moisture structure of the vortex is cylindrically symmetric about the storm center and defined by a moist adiabat that extends from 1000 hPa (with corresponding environmental temperature for that level) to a level where that moist adiabat intersects the environmental temperature sounding, which defines the cloud top. The relative humidity throughout the storm core is near 90%. The environmental parameters (including temperature) are obtained from an annular region with inner radius of R_{15} and outer radius of $2R_{15}$. This annulus is essentially the same annulus used as the blending zone for which the vortex is inserted into the environmental fields. This approach has been used for numerical studies of Hurricane Juan in 2003 by McTaggart-Cowan et al. (2006) and by Fogarty et al. (2006).

The initialization procedure described above is applied at 00/19 to the 12 km grids. This initial time was chosen when Michael was at its most developed *pre-transition* stage (Fig. 3b). It is important to apply the insertion before the onset of ET since the technique is most appropriate for hurricanes with a generally symmetric moisture structure, although we recognize that there are invariably some asymmetric features in all TCs. After the 12 km simulation is completed, a second integration on the 3 km grid (using output from the 12 km grid starting at 12/19) is run for 18 hours. The initial time of the 3 km simulations is 12 hours after the vortex insertion, which appears to be a suitable time for the model to "adjust" to the hurricane (e.g. spurious behavior in wind and pressure fields ceases after a

few hours of integration). The boundary conditions for the inner domain are updated every 30 minutes with output from the 12 km domain.[3] To reduce the possibility of "shocking" the model, we implant the synthetic vortex into the 12 km grid instead of the 3 km grid. This is also a desirable approach since the effects of the storm on the larger scale are resolved on the larger grid, which drives the 3 km grid used for resolving the details of the storm structure.

4. Control simulations

a. No-vortex simulation

We start by conducting a no-vortex simulation of this event (hereafter called NOVOR) on the "small" 12 km grid (see Fig. 6) beginning at 00/19 with a 42-hour integration length ending 18/20 and piloted by CMC analyses. We compare this with output from the regional GEM model forecasts for the same period. The GEM had a horizontal resolution of 24 km at the time of this event and was one of the primary sources of numerical guidance for weather forecasters during the storm. We will refer to this hereafter as GEM24.

With its relatively coarse resolution and scarcity of hurricane observations in the initial conditions, the GEM24 simply forecast a trough of low pressure at the location of

[3] MC2 is set up for one-way nesting only (from the outer domain to the inner domain)

Hurricane Michael. The model developed a baroclinic low south of Nova Scotia (the same low introduced earlier) and tracked it toward southwestern Newfoundland as shown in Fig. 7. The NOVOR simulation yielded a similar solution (see Fig. 7) with the baroclinic low being the dominant cyclone; however the model did generate a weaker low in the location of Hurricane Michael (not shown - this low was much too weak to be considered an adequate representation of the hurricane and tracked too far to the east over the Avalon Peninsula in eastern Newfoundland). Also in Fig. 7 we show the subjectively-analysed track of the baroclinic low for comparison (taken from Abraham et al. 2004).

The important difference between the observed track of the baroclinic low compared to the model results is that the observed low moves eastward between 12/19 and 18/19 while the GEM24 and NOVOR model runs show a motion toward the northeast close to the coast of Nova Scotia. This eastward motion occurs when the low becomes incorporated into the circulation of the hurricane – this was not captured by the GEM model. Surface weather data described by Abraham et al. (2004) suggest that the low may not have completely merged with the center of the hurricane (indicated by the northward turn in the track in Fig. 7); however it was clear that the hurricane became the dominant cyclone during the morning and afternoon of 19 October 2000.

b. Vortex-initiated control simulations

The control simulation for this event is one which applies the vortex insertion technique described in section 3. There are actually two control simulations – one on the small 12 km grid we call MICH12 and a second on the fine 3 km grid, which we call MICH3. For these runs, 14 km SST data from the National Environmental Satellite Data and Information Service (NESDIS) valid at 00/19 is used for the model ocean surface boundary condition. The SST remains fixed during the model integrations. The data is obtained from the NESDIS website at http://www.nesdis.noaa.gov/ and mapped to the piloting domain in Fig. 6a.

Simulated storm tracks are shown in Fig. 8a for MICH12 and in Fig. 8b for MICH3 including results from runs that use climatological SST (CLIM) at the lower boundary, which will be discussed briefly in section 5. Table 1 includes the vortex and model specifications for the 12 km control run. The remaining contents of the table refer to the ensemble system to be discussed in section 5. The overall track prediction is very good. The location of landfall is within 50 km of the actual landfall for both the 12 and 3 km runs. The timing of landfall is only 1 to 1.5 hours later than reality. The model reproduces the deceleration of the storm after landfall with an eastward motion during the day on 20 October as it was drifting with the deep-layered low shown in Fig. 3l.

Figure 9 displays time traces of minimum sea level pressure (MSLP), maximum surface wind (MSW) speed, and SST beneath the storm center for MICH12 and MICH3

simulations including the "best track"[4]. Before proceeding, we wish to clarify that when referring to the "best track", MSW is defined as the maximum one-minute mean (sustained) winds anywhere in the storm at 10 m above the surface (either estimated from satellite imagery or measured by aircraft). When referring to output from the model, MSW is the maximum instantaneous (e.g. snapshot) surface wind anywhere in the storm, where "surface" is defined at the 60-m (40-m) (e.g. lowest computational) level in the 12 km (3 km) simulations. Simulation hour zero in Fig. 9a-c corresponds to the time of synthetic vortex insertion. Focussing first on the MICH12 results we see that the model tends to deepen the storm from the start when in reality it weakened before undergoing rapid intensification after 6 hours (06/19). Given that the model requires approximately 12 hours adjusting to the new initial condition, we generally do not put much faith in the early part of the simulation. The model deepens the storm over the cooler waters and successfully represents the storm-central sea level pressure just prior to landfall. The modeled storm continues deepening to just below 960 hPa after landfall (~5 hPa deeper than reality) however the MSW is quite close to the observed winds during that period.

Results from the MICH3 control are also shown in Fig. 9a-c. One noticeable difference from MICH12 is that the MSW reaches 52 m s^{-1} (100 kts) in MICH3 compared to 47 m s^{-1} (91 kts) in MICH12. Both are overestimates of the observed MSW, which was near 44 m s^{-1} (85 kts). Regardless, this is much better than the NOVOR run which generated maximum winds of only 28 m s^{-1} (55 kts) at that time (not shown).

[4] Note that the best track is not exact, i.e., it is an estimate with inherent uncertainties on the order of ~±2.5 m s^{-1} for MSW and ~±4 hPa for MSLP throughout the lifecycle of the storm.

c. Impact of vortex insertion

We now examine the impact of employing the vortex insertion method in the model initial conditions compared to the no-vortex simulation discussed in subsection 4a. Fields of sea level pressure at 00/20 (24-hour prediction) are shown in Fig. 10 for GEM24, NOVOR, MICH12 and are compared with a manually drawn sea level pressure analysis (Fig. 10a). The NOVOR and GEM24 solutions clearly fail to capture the storm structure. The NOVOR run produces the baroclinic cyclone (discussed in subsection (a)) of 980 hPa just east of Nova Scotia and a weak (985 hPa) cyclone moving toward the Avalon Peninsula of Newfoundland. The eastern low is the model's poor interpretation of the hurricane. The experiment employing synthetic vortex insertion (MICH12) leads to a much different solution at 00/20 (Fig. 10d) with a 964-hPa storm just south of Newfoundland and an area of high winds on the east side of the low. This matches reasonably well with the analysis in Fig. 10a and with wind damage reports within about 200 km east of landfall. The no-vortex runs fail to produce this tight wind and pressure pattern.

d. Structural evolution during ET

A manually drawn sea level pressure analysis of Hurricane Michael at maximum intensity is shown in Fig. 11a. Model-simulated sea level pressure and surface (40 m)

wind speeds from the MICH3 simulation are shown in Fig. 11b for comparison. Simulated surface temperatures (40 m) are shown in Fig. 11c. Generally there is good agreement on the central pressure and overall storm circulation as depicted by the isobars - keeping in mind that the model time is one hour later to account for the ~1-hour delay of the simulated storm. Although the baroclinic low (which formed south of Nova Scotia) is represented in the model, it is not as close to the center of Michael as indicated in the analysis in Fig. 11a. We should add, however, that there is not enough data to confirm the actual location of the baroclinic low in Fig. 11a. Based on the work of Abraham et al. (2004), it was speculated that the low was not far to the southwest of Michael as shown by "L?" in Fig. 11a. The trough in SLP associated with the baroclinic low extends west of Michael in the model, while it is southwest of Michael in the analysis. Despite these differences, the hurricane is the dominant cyclone in the model during the early stage of ET.

The wind field around the center of Michael in Fig. 11b seems very realistic although we do not have enough surface wind observations to construct a 2D wind field for Fig. 11a. The MSW (at 40 m) at this time is 41 m s^{-1} (80 kts) 85 km to the south-southeast of the center. The magnitude is consistent with a ship report of 41 m s^{-1} measured 30 m above sea level approximately 20 km east of the storm center at 17/19 (keeping in mind the error in storm position is on the order of 25 km based on the analysis on page 1330 of Abraham et al. (2004)). This also suggests that the wind field was extremely "tight", which is represented in the simulation.

The presence of a significant background temperature gradient (i.e. baroclinic zone) showed in Fig. 11c highlights the extratropical nature of the environment. The warm front in the analysis in Fig. 11a is represented reasonably well in the simulation (but a bit further north) in Fig. 11c as denoted by the tight gradient in temperature and marked in the image. The storm would be considered as purely extratropical if the tight temperature gradient (front) extended into the center (as is the case with the baroclinic low in Fig. 11c).

Vertical profiles of wind speed taken approximately 85 km southeast of the hurricane center from a dropsonde (launched just prior to 17/19) and from the model (at 18/19) are shown in Fig. 12. For clarity, note that the horizontal distance from the launch position of the sonde and the surface center of the storm is ~85 km. The dropsonde profile exhibited the strongest low-level winds of any of the 16 sondes that were launched from the Convair 580 aircraft. The profile from the model was chosen as closely as possible to the storm-relative location of the dropsonde. The model profile was taken at 18/19 versus 17/19 in order to account for the slower simulated motion. Nonetheless, we can see that the surface wind speeds compare rather well, and the maximum low-level wind height is near 500 m in both. The model is unsuccessful in replicating the extreme low-level wind shear (at the very least, finer vertical resolution would be necessary to resolve this). The model does not capture the extreme wind magnitudes between 500 and 2000 m, which is also the case when sampling other vertical profiles from the model in the high wind region (not shown). On the other hand, the model does indicate that strong winds

extend through a deep layer of the atmosphere on the east side of the rapidly-moving storm.

Vertical cross sections of equivalent potential temperature (θ_e) and horizontal wind speeds from the MICH3 control experiment provide a summary of the thermodynamic and dynamic changes in the storm structure during ET in Fig. 13. The cross sections run from west to east through the center of the storm along a distance of 500 km. Panel (a) shows the structure of the initial idealized storm vortex. By 12/19 (Fig. 13b), ET has already begun as seen by the jet of low θ_e air on the west side of the storm. Drier air also intrudes into the mid levels of the storm (~500 hPa). As ET continues, the warm core (below 500 hPa) changes from having a westward tilt, to an eastward tilt prior to landfall, then to a northwestward tilt after landfall. This cannot be strictly discerned from the panels in Fig. 13, however, it *is* clear that the deep tropospheric tilt as a whole, is westward to northwestward, highlighting the extratropical nature of the cyclone. In addition, the strong wind jet encircling the storm contains increasingly cooler/drier air, effectively "secluding" the warm core from the cooler airmass to the north. This pattern was also observed in dropsonde data analyses (see contoured lobes of air with θ_e less than 330K in Fig. 10b of Abraham et al. 2004). The jet on the east side of the storm becomes elevated to near the 700 hPa level by 19/19 (Fig. 13d) and the warm core becomes thermodynamically decoupled from the cooler SSTs (~14^{o}C) as shown by the cool θ_e air in the lower BL. In the hours leading up to landfall, drier air intrudes into the midlevels of the storm and destroys the upper part of it (Fig. 13e). Just prior to landfall (Fig. 13f)

very low θ_e air (< 310 K) floods in from the west and the storm becomes frontal, although an elevated warm core remains.

5. Sensitivity experiments

a. Summary of the ensemble system

An ensemble of 17 experiments is run on the 12 km grids shown in Fig. 6 for Hurricane Michael to provide a measure of storm sensitivity to various initial and boundary conditions, as well as model parameters. A summary of the members of the ensemble is displayed in Table 1. The control experiment piloted by CMC analyses on the small 12 km grid is denoted by "MICH" in the table. Experiments "MICH_GSM" and "MICH_GLG" represent experiments piloted by GEM forecast fields on the small and large 12 km grids, respectively. All other members in the ensemble are run on the small 12 km piloted by analyses from the CMC Data Assimilation System archive (Chouinard et al. 1994).

One of the vortex parameters that can be tuned is the percentage of the background flow used as a proxy for the wind field asymmetry and maximum surface winds in the initial specified vortex for a given MSLP. The default value is 50% but we run two ensemble members whereby the value is changed to 25% and 75%. The corresponding initial

maximum surface wind speeds for 25, 50 and 75% are 34, 38 and 41 m s^{-1} respectively. These values represent a realistic range in the observed storm intensity (typically ±5-10 knots in MSW or ±2.5-5 m s^{-1}). Choosing 50% yields a value closest to the observed (best track) intensity of 39 m s^{-1} at 00/19.

The second set of ensemble members involves adjustment of the initial vortex size. The size is given by the radius of the 15 m s^{-1} isotach (R_{15}). In the control experiments we use 320 km, which was determined by scaling the mean gale radius included in the NHC bulletins archive (http://www.nhc.noaa.gov/archive/2000/MICHAEL.html).

An additional pair of members is generated by adjusting the initial storm intensity, which is done through perturbation of the MSLP. At 00/19 (the start time of the model) the MSLP of Michael was estimated to be 983 hPa, but the error in that value is approximately ±4 hPa, so we use that as a basis for the pair (979 hPa and 987 hPa). Four more members are generated by perturbing the initial storm location by 74 km (~six grid points) in each cardinal direction. The advertised positional error for Michael at 00/19 was 40 nm (74 km) based on information from the NHC bulletin archive.

The convective scheme is switched from Kain and Fritsch (1990) in the control run to Fritsch and Chappel (1980) for one member and to Kuo (1974) for another to examine the sensitivity of the storm simulations to the choice of convective parameterization. Vertical resolution was increased from 25(7) levels in the control run to 35(10) comprising another member of the ensemble suite (number of BL levels below 1500 m is

shown in parentheses). The final member in the suite employs the cloud microphysical scheme of Kong and Yau (1997). The default (control) microphysical scheme in the simulations follows that of Tremblay et al. (1996).

A composite of simulated storm tracks from the 17-member ensemble plus the control run is shown in Fig. 14. The tracks are clustered fairly closely together with no significant outliers. The degree of spread in tracks with time is also quite small. This is likely owing to the fact that the atmospheric steering flow is very strong and there is not a lot of time for the storm to deviate from the control solution. The mean 24-hour error in storm position (valid time 00/20 near landfall) for the ensemble was 161 km. The 24-hour CHC operational forecast position for Michael (valid at 00/20) was 47^{o}N, 60^{o}W with maximum surface winds near 28 m s^{-1} (55 kts) and central pressure of 994 hPa. This corresponds to an error in the track forecast of 400 km and intensity error of 11 m s^{-1} (20 kts) and 28 hPa too high (compared to the best track) in terms of central pressure, highlighting the difficulty in forecasting this event. Incidentally, subsequent forecasts did improve once it became clear what was happening.

The ensemble means for MSLP and MSW are shown in Fig. 15 compared with the best track. The ensemble means do not differ significantly from the control run (Figs. 7a and 7b), but here we can see the degree of variability among ensemble members as indicated by the one-standard deviation range bars in the plots in Fig. 15. There is a significant amount of variability in MSLP that grows with time during the first 15 hours of the experiments. In terms of MSW, the degree of variability is greatest between simulation

hours 9 and 18. Incidentally this corresponds very closely to the period when Michael was undergoing ET. The variability then drops after 18 hours and is relatively small after 24 hours, which corresponds to the extratropical phase of the storm. The landfall intensity in terms of wind speed at simulation hour 24 does not appear to be highly sensitive to the perturbed initial conditions and model parameters. Much of the variability during the ET period occurs among members employing different convective and cloud microphysical schemes. Note that the variability among members of the ensemble is not enough to explain the rapid intensification period observed between 15 and 18 hours (in terms of MSLP). This is not a surprise since it is well known that numerical models have difficulty forecasting sudden changes in the intensity of tropical cyclones, given that the processes governing these changes occur at scales unresolved by the model (Krishnamurti et al. 2005).

b. Sensitivity to driving fields and domain size

The experiments examined so far in this paper were driven by large scale analyses fields which represent the "best" boundary conditions available. However, in order to obtain a better idea of model performance for this case in a forecast mode of operation, driving fields from a regional forecast model are used (in this case, from the GEM model). We also test a larger 12 km domain (shown in Fig. 6).

Resulting post-landfall (27HR) sea level pressure and 1000-hPa wind speed analyses from these experiments are summarized in Fig. 16. The control run (MICH12) result is shown in Fig. 16a. Results from the MICH_GSM and MICH_GLG (GEM-piloted) runs are shown in Fig. 16b and Fig. 16c, respectively. Finally, the resulting sea level pressure and wind analysis from the GEM-piloted NOVOR experiment is shown in Fig. 16d. The general result from these experiments is that the vortex-initiated runs lead to a single, deep area of low pressure over central or eastern Newfoundland, with an area of strong winds over the eastern part of the island. However, there are differences in the storm structure, position and intensity that are dependant on the driving fields and domain size. As one might expect, the GEM-piloted runs are not as accurate as the analyses-driven run, and interestingly, the simulation on the larger 12 km grid is slightly worse than on the smaller grid.

It is reasonable to expect the solutions from the GEM-piloted runs to be of lesser quality than those driven by analyses. It is perhaps less obvious that the storm location from the larger 12 km simulation is less accurate than that from the smaller one. To investigate this further, we ran the large and small 12 km grids without vortex insertion for comparison. Slight differences in the evolution of the 500-hPa geopotential height pattern were noted (not shown) as well as notable differences in the sea level pressure field throughout the domain. When comparing the differences in these fields for the MICH_GSM and MICH_GLG runs, similar differences were observed in the far field (as well as near the storm centers) as were seen in the no-vortex comparison. It appears that the different solution for the large domain is not attributable to the vortex insertion, but is

most likely owing to the position of propagating features at the edge of the domains at the beginning of the simulations (Landman et al. 2005). In a test case where we pilot the small 12 km grid with output from the large (not shown), we notice no difference in the output of fields in the overlapping region. This indicates compliance with the "acid test", also as demonstrated in section 7c of Thomas et al. (1998). The bottom line from this comparison is that a larger grid does not necessarily equate to an improved hindcast/forecast.

c. Comparison with operational guidance

A summary of operational numerical model track and intensity forecasts issued at 00/19 is shown in Fig. 17 and Fig. 18. Shown in this operational suite of guidance is the Florida State Superensemble (SENS) which contains information from various dynamical models to produce a weighted ensemble mean (weighting being proportional to the past performance of model members) as described by Williford et al. (2003). Also shown are the UKMET and GFDL models, which were introduced in section 1. The CHC and NHC forecasts are based on a forecaster's "blend" of all available guidance including the dynamical models shown in the figures. Finally, the results from the MICH_GSM experiment (labeled MC2) is shown since it mimics the forecast mode of operation. The point we wish to make here is that the MC2 falls within the range of other dynamical models and guidance, suggesting that even simple vortex insertion prior to the ET of Michael in forecast mode would provide useful guidance to forecasters.

d. Sensitivity to SST

As a final sensitivity experiment, we conduct simulations identical to MICH12 and MICH3 using climatological SST from Geshelin et al. (1999). The climatology is organized into monthly means, which are used to find the equivalent climatology for 19 October using a weighted average of October and November data. The data have a resolution of 18.5 km and are interpolated to the 28-km "piloting" domain for the model (see Fig. 6). A map showing the observed minus climatology SST (anomaly) with the storm track is shown in Fig. 19. The SSTs were near normal south of ~40^{o}N and anomalously warm north of that along the storm track, with the largest anomaly of 3-4^{o}C near 43^{o}N.

Results from the climatology SST runs (CLIM12 and CLIM3) are shown in Fig. 8 and Fig. 9. The impact on storm track is negligible, especially when compared with the variability in tracks from the ensemble system. There appears to be some impact on storm intensity, but the signal is not as significant as that observed during similar experiments with Hurricane Juan while approaching Nova Scotia in September, 2003 (Fogarty et al. 2006). For instance, there is not a great difference in MSLP and MSW between the MICH3 and CLIM3 at the time of landfall (see Fig. 9a and Fig. 9b). The only difference in MSW that appears significant occurs during the high resolution runs (MICH3 and CLIM3) between 14 and 18 hours. This corresponds to the period when the

simulated storm travelled between 40 and 43°N over the warm SST anomalies shown in Fig. 19.

As noted above, the landfalling intensity is not overly sensitive to the (relatively) small departures of SSTs from climatology. This is not surprising since the synoptic environment is most conducive to baroclinic intensification of the storm, as opposed to tropical-type intensification (through oceanic heat transfer).

6. Summary and conclusions

A mesoscale model of the atmosphere was used to simulate the extratropical transition (ET) of Hurricane Michael during its approach to Newfoundland in October 2000. A synthetic three-dimensional hurricane vortex was constructed prior to running the model and used to replace the poorly represented cyclone in the large-scale analysis fields. The improved initial conditions allowed for much more realistic simulations of the storm than was the case without inserting a synthetic vortex. The model was used to diagnose the structural changes of Hurricane Michael during ET and to study the sensitivity of hindcast simulations to various initial conditions, lateral driving fields, domain sizes and model parameters.

During Michael's early stage of ET, the model successfully simulated the absorption of a baroclinic cyclone into the hurricane circulation. On the other hand, when a hurricane

vortex was not used in the initial conditions, the baroclinic cyclone became the dominant circulation. During the actual event, forecasters were not sure which scenario would materialize until approximately six hours before landfall. We suggest that the model would be a valuable forecast tool during situations such as this, particularly when the tropical cyclone is poorly represented in the model initial conditions. Simulations from the present study were driven by synoptic-scale analyses which is obviously not possible when employing the model as a predictive tool. Nonetheless, a "pseudo-forecast" (piloted by synoptic-scale numerical weather forecasts) conducted as a test for Hurricane Michael lead to improved representation of the storm lifecycle as in the simulations piloted by analyses. The "pseudo forecast" also compared well with operational guidance available during the event.

The model simulated the intensification of Michael within a baroclinic environment while traversing sea surface temperatures less than 26^{o}C. When run at 3 km resolution and driven by large scale analyses, the model produced realistic storm intensity at landfall with central pressure of 967 hPa (compared to observed pressure of 966 hPa) and maximum surface winds of ~36 m s^{-1} (compared to observed winds of ~39 m s^{-1}).

Aircraft measurements of Hurricane Michael showed the presence of a deep layer of strong winds on the southeastern side of the storm. The model also simulated this structure, but the modeled winds were not as intense as the observed winds. Aircraft, satellite and radar data indicated that Michael was tilted toward the east or northeast prior to landfall, at least below the 500-hPa level. The model showed storm tilt toward the

northwest originally then toward the east and northeast during its approach to southern Newfoundland, which was consistent with the observed tilt during that time.

Variability in storm intensity (in terms of maximum wind speeds) among the sensitivity experiments was greatest during the ET phase of the storm while it was much less during the extratropical phase. The simulations were sensitive to choice of lateral piloting fields (analyses versus forecasts) and to the choice of domain size. The model was not able to simulate the most rapid period of intensification (in terms of central sea level pressure) but this is a common problem with numerical models, and in this case, did not have a significant influence on the landfalling intensity of the storm in Newfoundland.

When testing the role of warm sea surface temperature (SST) anomalies along the track of Michael by running a climatological SST simulation, the intensity appeared sensitive to the local SST anomaly between 40^{o} and 43^{o}N (~2.5-5 m s^{-1} weaker winds than in the control run) yet there was no significant impact on storm intensity at or following landfall. The degree of spread among the ensemble members was comparable to the spread among various operational dynamical models, making the MC2 (with simple vortex insertion) a potential operational forecasting tool for short-range prediction of hurricanes undergoing ET in Eastern Canada.

Acknowledgements

REFERENCES

Abraham, J., W. Strapp., C. Fogarty, and M. Wolde, 2004: Extratropical transition of Hurricane Michael: an aircraft investigation. *Bul. Amer. Meteor. Soc*., **85,** 323–1339.

Agusti-Panareda, A., C. D. Thorncroft, G. C. Craig, and S. L. Gray, 2004: The extratropical transition of Hurricane Irene (1999): a potential-vorticity perspective. *Q. J. R. Meteorol. Soc.*, **130**, 1047-1074.

Benoit, R., M. Desgagné, P. Pellerin, S. Pellerin, S. Desjardins and Y. Chartier, 1997: The Canadian MC2: a semi-Lagrangian, semi-implicit wide-band atmospheric model suited for fine-scale process studies and simulation. *Mon. Wea. Rev*., **125**, 2382-2415.

———, and J. Mailhot, 1989: Inclusion of a TKE boundary layer parameterization in the Canadian regional finite-element model. *Mon. Wea. Rev.*, **117**, 1726-1750.

Chouinard, C., J. Mailhot, H. L. Mitchell, A. Staniforth, and R. Hogue, 1994: The Canadian regional data assimilation system: Operational and research applications. *Mon. Wea. Rev* ., **122**, 1306-1325.

Colle, B. A., 2003: Numerical simulations of the extratropical transition of Floyd (1999): structural evolution and responsible mechanisms for the heavy rainfall over the northeast United States. *Mon. Wea. Rev.*, **131**, 2905–2926.

Davidson, N. E., J. Wadsley, K. Puri, K. Kurihara, and M. Ueno, 1993: Implementation of the JMA typhoon bogus in the BMRC tropical prediction system. *J. Met. Soc. Japan*, **71**(4), 437-467.

———, and H. C. Weber, 2000: The BMRC high-resolution tropical cyclone prediction system: TC-LAPS. *Mon. Wea. Rev.,* **128**, 1245-1265.

Davis, C. A., and L. F. Bosart, 2003: Baroclinically induced tropical cyclogenesis. *Mon. Wea. Rev.,* **131**, 2730–2747.

Evans, J. L., J. M. Arnott, and F. Chiaromonte, 2006: Evaluation of operational model cyclone structure forecasts during extratropical transition. *Mon. Wea. Rev.,* (in press).

———, and R. E. Hart, 2003: Objective indicators of the life cycle of extratropical transition for Atlantic tropical cyclones. *Mon. Wea. Rev*., **131**, 909-925.

Fogarty, C. T., R. J. Greatbatch, and H. Ritchie, 2006: The role of anomalously warm sea surface temperatures on the intensity of Hurricane Juan (2003) during its approach to Nova Scotia. *Mon. Wea. Rev*., **134**, 1484-1504.

Frank, W. M., and E. A. Ritchie, 1999: Effects of environmental flow upon tropical cyclone structure. *Mon. Wea. Rev.,* **127**, 2044-2061.

Fritsch, J. M., and C. F. Chappel, 1980: Numerical prediction of convectively driven mesoscale pressure systems. Part I: Convective parameterization. *J. Atmos. Sci.,* **37**, 1722-1733.

Fujita, T., 1952: Pressure distribution within a typhoon. *Geophys. Mag.,* **23**, 437-451.

Gal-Chen, T., and R. Somerville, 1975: On the use of a coordinate transformation for the solution of the Navier-Stokes equations. *J. Comput. Phys.,* **17**(2), 209-228.

Geshelin, Y., J. Sheng, and R. J. Greatbatch, 1999: Monthly mean climatologies of temperature and salinity in the western North Atlantic. Can. Tech. Rep. Hydrogr. Ocean. Sci. 153: vi+62 pp.

Hart, R.E., 2003: A cyclone phase space derived from thermal wind and thermal asymmetry. *Mon. Wea. Rev.*, **131**, 585-616.

———, and J. L. Evans, 2004: Synoptic composites of the extratropical transition lifecycle of North Atlantic TCs as defined within cyclone phase space. Preprints, *26th Conf. on Hurricanes and Tropical Meteorology,* Miami Beach, FL, Amer. Meteor. Soc., 681-682.

Heming, J. T., and A. M. Radford, 1998: The performance of the United Kingdom Office Global Model in predicting the tracks of Atlantic tropical cyclones in 1995. *Mon. Wea. Rev.,* **126**, 1323-1331.

Jones, S. C., P. A. Patrick, J. Abraham, L. F. Bosart, P. J. Bowyer, J. L. Evans, D. E. Hanley, B. N. Hanstrum, R. E. Hart, F. Lalaurette, M. R. Sinclair, R. K. Smith, and C. Thorncroft, 2003: The extratropical transition of tropical cyclones: forecast challenges, current understanding, and future directions. *Wea. and Forecasting*, **18**, 1052–1092.

Kain, J. S., and J. M. Fritsch, 1990: A one-dimensional entraining/detraining plume model and its application in convective parameterization. *J. Atmos. Sci.,* **47**, 2784-2802.

Kimball, S. K., and J. L. Evans, 2002: Idealized numerical simulations of hurricane-trough interaction. *Mon. Wea. Rev.,* **130**, 2210-2227.

Klein, P. M., P. A. Harr, and R. L. Elsberry, 2002: Extratropical transition of western North Pacific tropical cyclones: midlatitude and tropical cyclone contributions to reintensification. *Mon. Wea. Rev.*, **130**, 2240-2259.

Kong, F., and M. K. Yau, 1997: An explicit approach of microphysics in MC2. *Atmosphere-Ocean*, **35**, 257-291.

Krishnamurti, T. N., S. Pattnaik, L. Stefanova, T. S. V. Kumar, B. P. Mackey, A. J. O'Shay and R. J. Pasch, 2005: The Hurricane Intensity Issue. *Mon. Wea. Rev.*, **133**, 1886–1912.

Kuo, H. L., 1974: Further studies on the parameterization of the influence of cumulus convection on large-scale flow. *J. Atmos. Sci.*, **31**, 1232-1240.

Kurihara, Y., M. A. Bender, R. E. Tuleya, and R. J. Ross, 1995: Improvements in the GFDL hurricane prediction system. *Mon. Wea. Rev.,* **123**, 2791-2801.

Landman, W. A., A. Seth, and S. J. Camargo, 2005: The effect of regional climate model domain choice on the simulation of tropical cyclone–like vortices in the Southwestern Indian Ocean. *J. of Climate*, **18**, 1263-1274.

McTaggart-Cowan, R., J. R. Gyakum, and M. K. Yau, 2001: Sensitivity testing of extratropical transitions using potential vorticity inversions to modify initial conditions: Hurricane Earl case study. *Mon. Wea. Rev.,* **129**, 1617–1636.

———, L. F. Bosart, E. Atallah, J. R. Gyakum, and L. F. Bosart, 2006: Hurricane Juan (2003). Part II: Forecasting and numerical simulation. *Mon. Wea. Rev*., **134**, 1748-1771.

Monin, A. S., and A. M. Obukhov, 1954: Basic laws of turbulent mixing in the surface layer of the atmosphere. *Tr. Geofiz. Inst. Akad. Nauk SSSR,* **151**, 163-187.

Ritchie, E. A., and R. L. Elsberry, 2001: Simulations of the transformation stage of the extratropical transition of tropical cyclones. *Mon. Wea. Rev.*, **129**, 1462-1480.

Stewart, S. R., 2000: Tropical cyclone report for Hurricane Michael: 17-19 October 2000. NCEP Rep., 13 pp. [Available online at: http://www.nhc.noaa.gov/2000michael.html]

Thomas, S. J., C. Girard, R. Benoit, M. Desgagné, and P. Pellerin, 1998: A new adiabatic kernel for the MC2 model. *Atmosphere-Ocean*, **36**, 241-270.

Tremblay, A. A., W. Yu, and R. Benoit, 1996: An explicit cloud scheme based on a single prognostic equation. *Tellus.*, **48A**, 483–500.

Williford, C. E., T. N. Krishnamurti, R. C. Torres, S. Cocke, Z. Christidis, and T. S. Vijaya Kumar, 2003: Real-time multimodel superensemble forecasts of Atlantic tropical systems of 1999. *Mon. Wea. Rev.*, **131**, 1878-1894.

List of figures

Figure 1. Storm track (best track) for Hurricane Michael with sea surface temperatures valid 00/19 (every 2^{o}C). Times shown are of the form HH/DD UTC.

Figure 2. Time series history for Hurricane Michael: minimum sea level pressure (hPa; thick line), maximum sustained wind speed (m s^{-1}; medium line), and storm forward speed (m s^{-1}; thin line). Values in parentheses at the bottom of the plot indicate sea surface temperatures (^{o}C) beneath the storm center.

Figure 3. Evolution of GOES infrared satellite and 500-hPa geopotential height and absolute vorticity analyses during the extratropical transition of Hurricane Michael, Oct. 2000. The location of Michael in the satellite images is marked with a white "M" where not obvious, and the baroclinic low with a black L. The location of the hurricane surface center in the 500-hPa panels is shown by the large black asterisk.

Figure 4. Hurricane Michael ET as represented within cyclone phase space using 1° AVN analyses. The ordinate indicates the storm symmetry (B) while the abscissa is a measure of the cold-/warm-core structure of the system (rhs of diagram corresponds to $-|\mathbf{V}^{L}_{T}| > 0$ for warm core) as described in Hart (2003). Time moves forward from A and Z, the start and end of the cyclone life cycle resolvable within the available dataset and its geographic boundaries. The size of the cyclone (mean radius of the 925-hPa gale force winds) corresponds to the size of the solid circles along the phase trajectory (largest

shown is approximately 750 km). Circle color corresponds to the intensity of the cyclone, with purple for the weaker end of the scale and green for the more intense. The track of the cyclone is plotted in the inset, with the date marked at the 0000 UTC positions.

Figure 5. Manually drawn (subjective) sea level pressure analysis (contours every 4 hPa) of Hurricane Michael and the baroclinic cyclone at 12/19. Standard synoptic weather data plots are also shown.

Figure 6. Layout for the model experiments. (a) grid configurations and (b) timelines for the model integrations. The asterisk in (a) marks the storm center at time-zero of the 12-km control simulations and the open circle marks the mean position of the storm at time-zero of the 3-km control simulations. The grey region on the 12-km timeline in (b) denotes the 12-hour model adjustment period.

Figure 7. Tracks of the baroclinic cyclone center from observations (OBSVD), the operational GEM model (GEM24), and the no-vortex version of the MC2 model (NOVOR) every three hours from 06 UTC 19 October to 00 UTC 20 October. The best track (BT) segment during the period of interest is also plotted. The valid time for the storm positions in UTC is indicated to the lower right of the position markers.

Figure 8. (a) Storm tracks from the 12 km control, and (b) 3 km control runs of the model. Black trajectories denote the "best track", red trajectories denote the observed-SST control run, and green is the climatology SST storm track. Track nodes are every

three hours in (a) from 00/19 to 18/20 and every hour in (b) from 12/19 to 06/20. Observed (NESDIS) SST (every 1^{o}C) is also shown.

Figure 9. Model results for the 12-km control (MICH12 and CLIM12) and 3-km control (MICH3 and CLIM3) simulations: (a) evolution of minimum sea level pressure (MSLP) for MICH12 (thin red line), CLIM12 (thin green line), MICH3 (thick red line), CLIM3 (thick green line) and the best track (black line); (b) maximum surface winds (MSW); and (c) sea surface temperature (SST) beneath the storm center as a function of model simulation time (hours). The vertical bars in (a) denote the approximate model landfall time (blue) and observed landfall time (black).

Figure 10. Sea level pressure (every 4 hPa) valid at 00 UTC 20 October based on: (a) manually drawn (subjective) analysis, (b) 24-hour GEM regional forecast, (c) 24-hour "no-vortex" simulation of the 12-km MC2 model, and (d) 24-hour simulation of the control run of the MC2 model with vortex insertion employed (MICH12). Standard synoptic weather plots are shown in (a).

Figure 11. (a) Manually drawn (subjective) sea level pressure (every 4 hPa) valid at 18/19; (b) 3-km model control simulation (MICH3) valid at 19/19 showing sea-level pressure (solid grey contours) and surface (40 m) wind speed (shaded) every 4 m s^{-1}; and (c) same as (b) except with model-simulated surface (40m) temperatures (shaded every 2^{o}C). The estimated position of the baroclinic cyclone in (a) is shown by "L?" and is also marked in (b) and (c).

Figure 12. Vertical profiles of horizontal wind speed from aircraft dropsonde #8 at 17/19 and 3-km run of the model (MICH3) at 18/19. The storm-relative position of the profiles is 85 km southeast of the surface position of the hurricane.

Figure 13. Vertical cross sections of equivalent potential temperature (colored field) and horizontal wind speed magnitude (solid contours every 10 knots – 1 knot = 0.515 m s^{-1}) from the 3-km control simulation (MICH3) at selected times during extratropical transition. The cross sections are taken along a west to east line through the storm center. Panel (a) shows the structure of the synthetic vortex at 00/19.

Figure 14. Storm tracks for all ensemble members (including control) from the set of simulations in Table 1 (black), plus the best track (grey). Track positions are every three hours for the 42-hour period from 00/19 to 18/20 October.

Figure 15. (a) Minimum sea level pressure, and (b) maximum surface wind traces for the ensemble mean (thick curve) and the best track (thin curve). Vertical range bars denote the one-standard deviation values from the ensemble.

Figure 16. Sea level pressure (black contours) and 1000-hPa wind field (shaded) at simulation hour 27 from the domain and driving-field experiments: (a) small 12 km grid experiment piloted by analyses (MICH12), (b) small 12 km grid experiment piloted by GEM forecasts (MICH_GSM), (c) large 12 km grid experiment piloted by GEM

forecasts (MICH_GLG), and (d) small 12 km grid experiment without vortex insertion piloted by GEM forecasts (NOVOR_GSM). Sea level pressure interval is 4 hPa and 1000-hPa wind speed is every 5 kts, where 1 kt = 0.515 m s^{-1}.

Figure 17. Operational and numerical track forecasts for Hurricane Michael for a 36-hour period beginning 00/19. The acronyms in the legend are defined in the text.

Figure 18. Operational and numerical intensity forecasts in terms of maximum sustained (surface) winds (MSW) for Hurricane Michael for a 36-hour period beginning 00/19. The acronyms in the legend are defined in the text.

Figure 19. Sea surface temperature anomaly valid at 00 UTC 19 October 2000 (every 1^{o}C). Negative anomaly is represented by dotted contours. Partial storm track for Hurricane Michael also shown.

Table caption

Table 1. List of experiments used in the study with the 12-km grid. MICH12 is the control run using 19 October observed SST surface boundary condition. MICH_GSM and MICH_GLG are the experiments whose lateral boundaries are driven by GEM output fields. Minimum sea level pressure is MSLP, lat/lon indicate the storm center position, R15 is the radius of 15 m s^{-1} winds, "basicp" is the fraction of the background flow used to prescribe the initial wind field asymmetry, "convec" is the convective parameterization scheme, "comp_levs" indicates the number of computational levels in the model, and "stcond" is the stratiform condensation scheme (schemes are explained in the text). Changed parameters in each experiment are in bold italics.

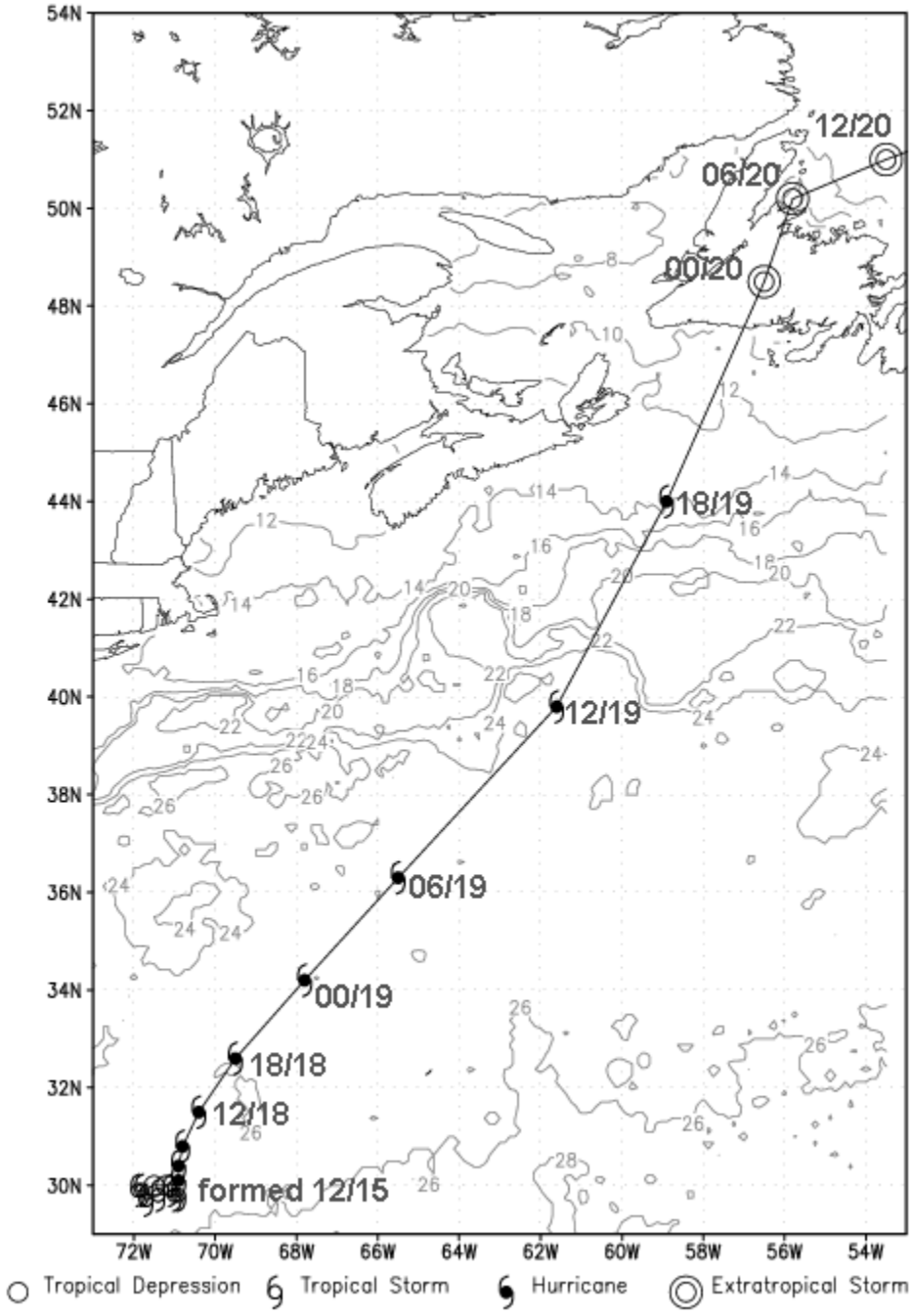

Figure 1. Storm track (best track) for Hurricane Michael with sea surface temperatures valid 00/19 (every 2°C). Times shown are of the form HH/DD UTC.

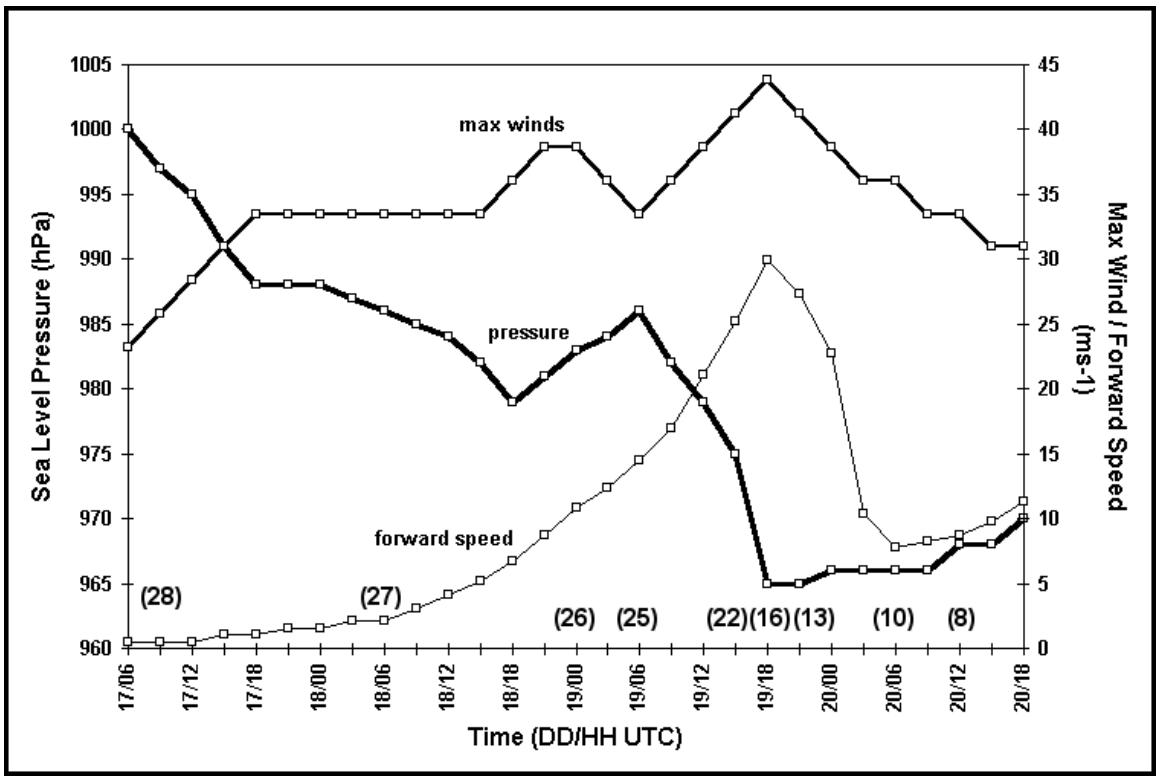

Figure 2 Time series history for Hurricane Michael: minimum sea level pressure (hPa; thick line), maximum sustained wind speed (m s^{-1}; medium line), and storm forward speed (m s^{-1}; thin line). Values in parentheses at the bottom of the plot indicate sea surface temperatures (^{o}C) beneath the storm center.

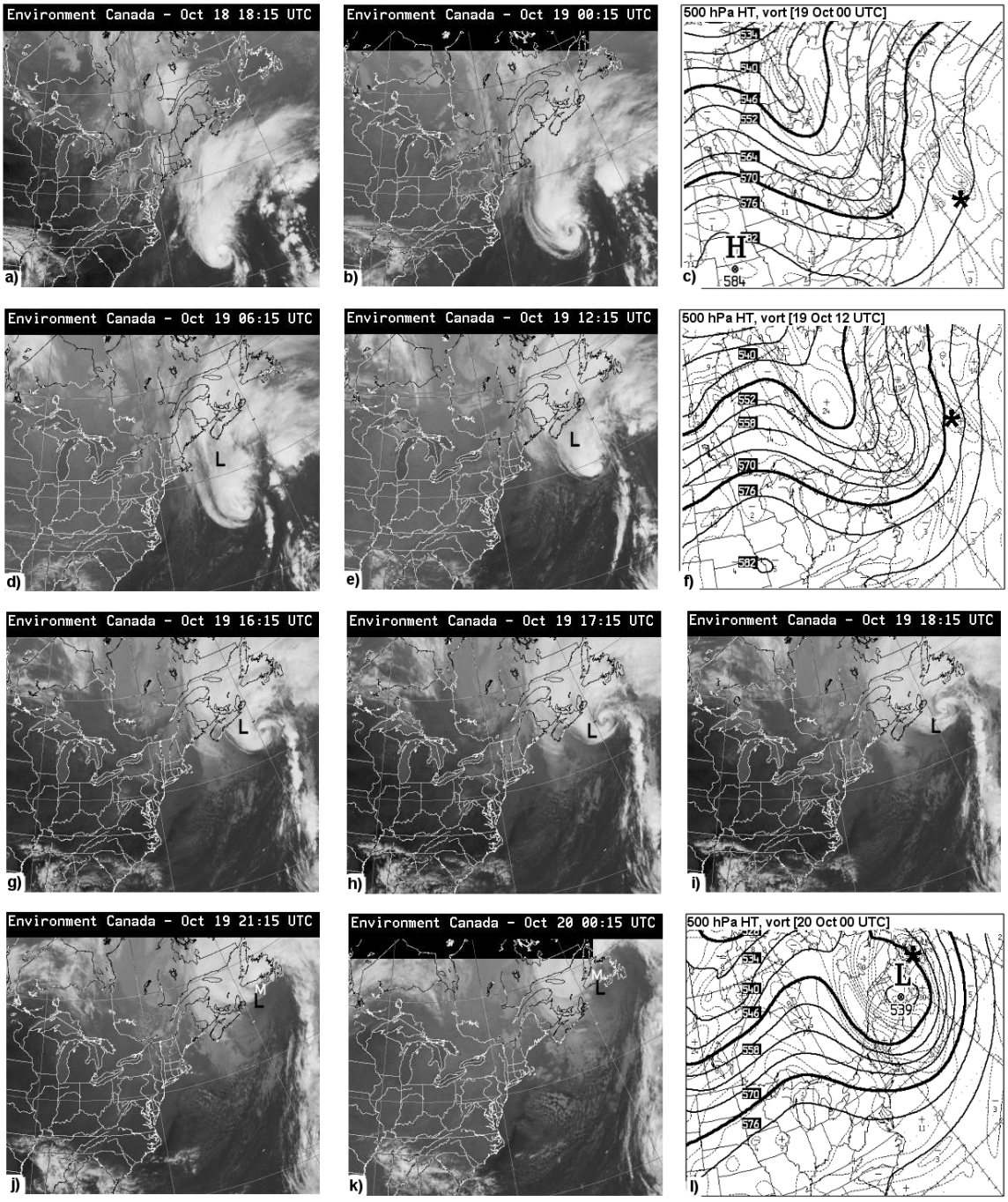

Figure 3. Evolution of GOES infrared satellite and 500-hPa geopotential height and absolute vorticity analyses during the extratropical transition of Hurricane Michael, Oct. 2000. The location of Michael in the satellite images is marked with a white "M" where not obvious, and the baroclinic low with a black L. The location of the hurricane surface center in the 500-hPa panels is shown by the large black asterisk.

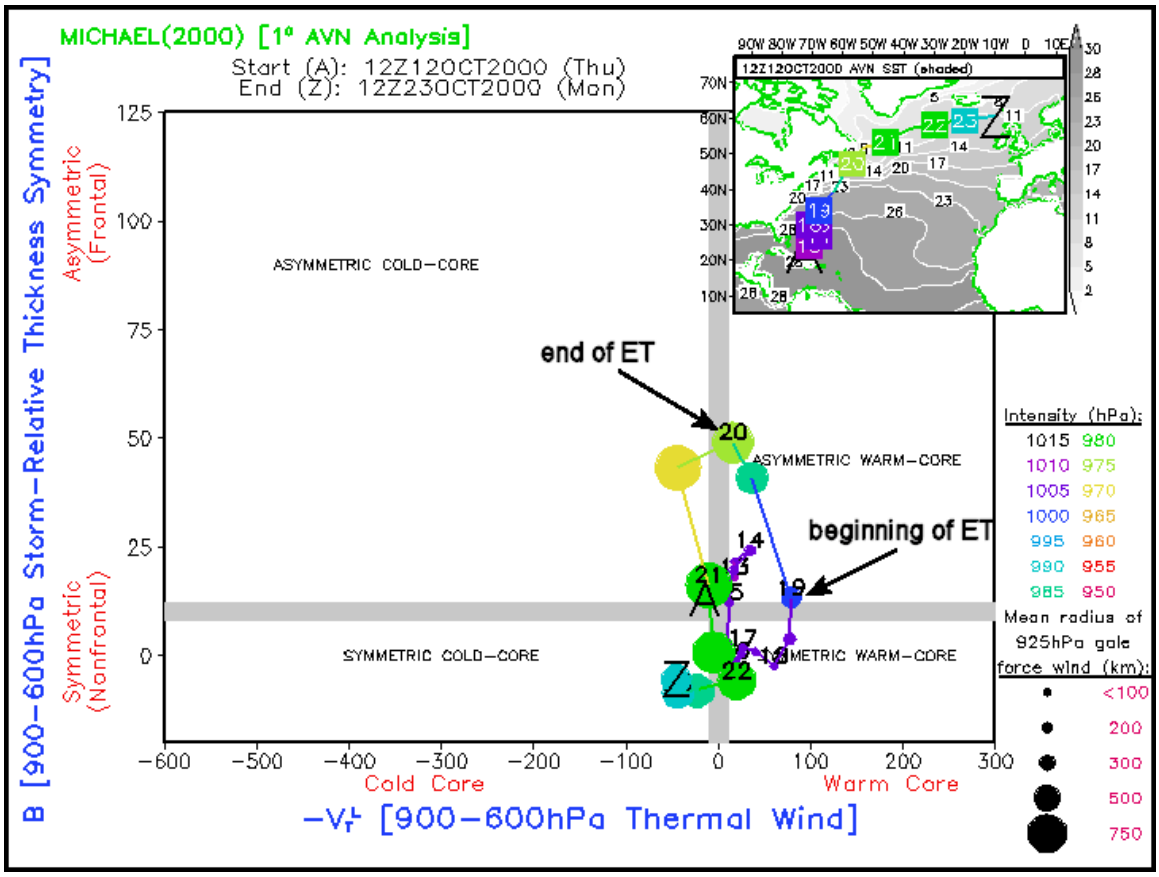

Figure 4. Hurricane Michael ET as represented within cyclone phase space using 1° AVN analyses. The ordinate indicates the storm symmetry (*B*) while the abscissa is a measure of the cold-/warm-core structure of the system (rhs of diagram corresponds to $-|\mathbf{V}^{L}_{T}| > 0$ for warm core) as described in Hart (2003). Time moves forward from A and Z, the start and end of the cyclone life cycle resolvable within the available dataset and its geographic boundaries. The size of the cyclone (mean radius of the 925-hPa gale force winds) corresponds to the size of the solid circles along the phase trajectory (largest shown is approximately 750 km). Circle color corresponds to the intensity of the cyclone, with purple for the weaker end of the scale and green for the more intense. The track of the cyclone is plotted in the inset, with the date marked at the 0000 UTC positions.

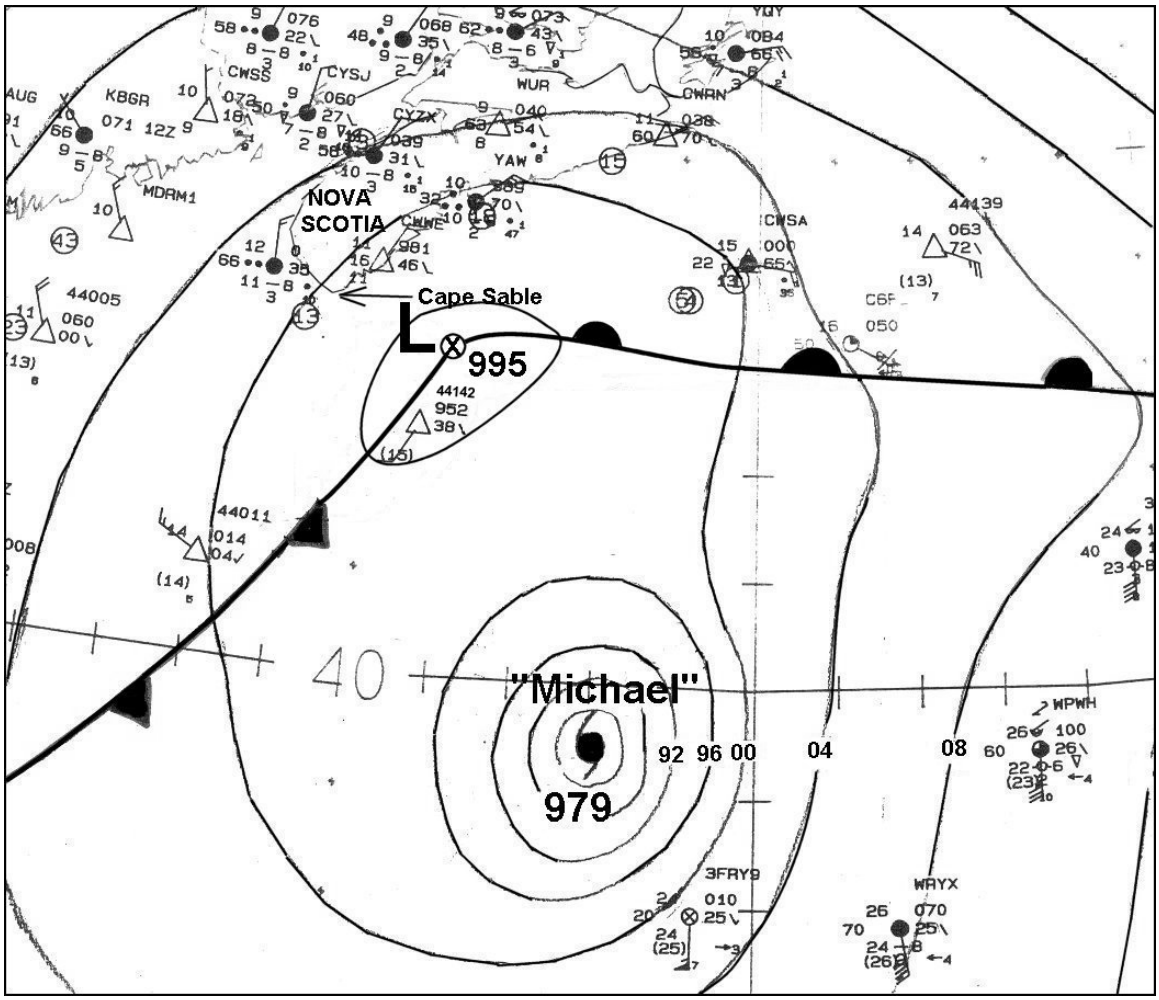

Figure 5. Manually drawn (subjective) sea level pressure analysis (contours every 4 hPa) of Hurricane Michael and the baroclinic cyclone at 12/19. Standard synoptic weather data plots are also shown.

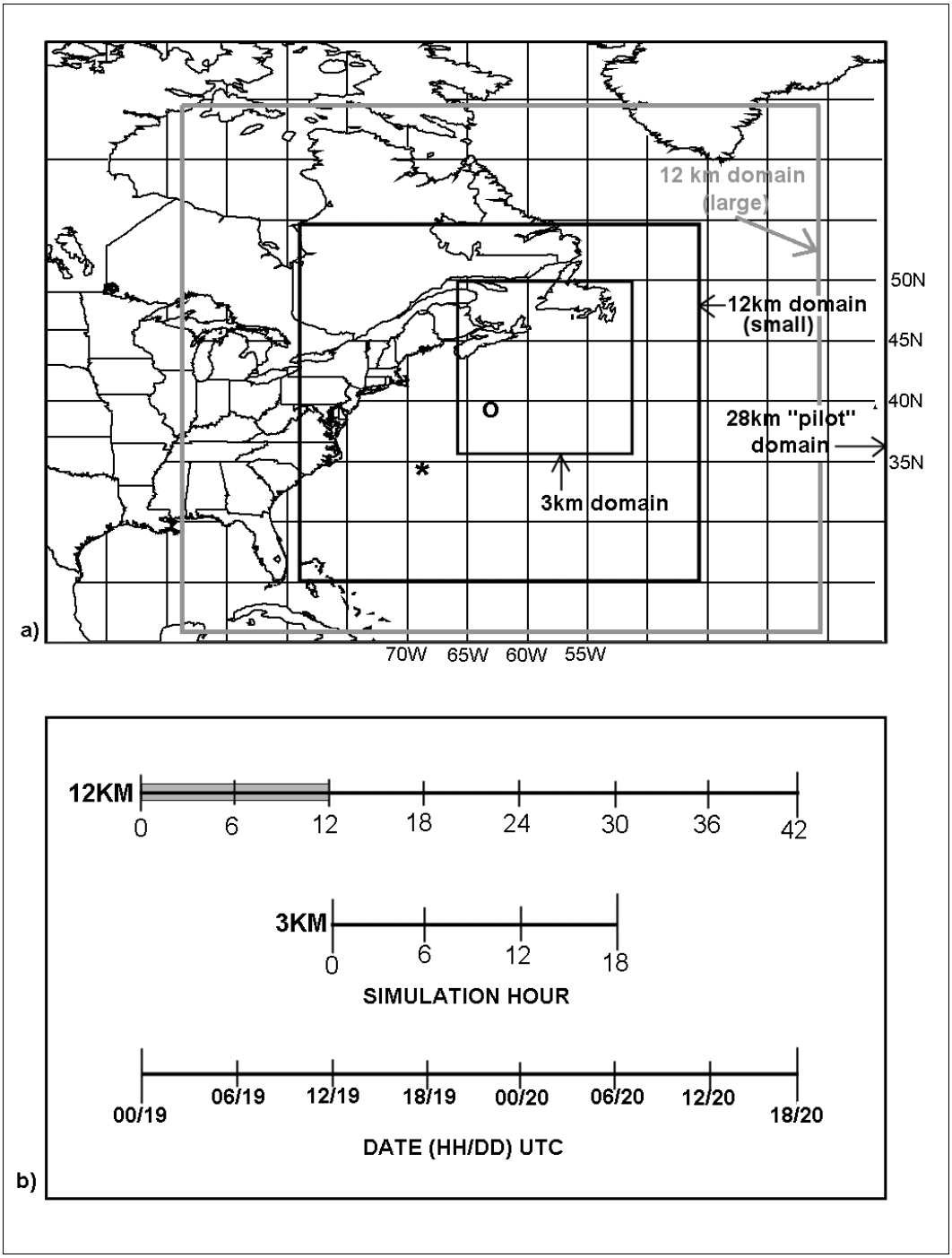

Figure 6. Layout for the model experiments. (a) grid configurations and (b) timelines for the model integrations. The asterisk in (a) marks the storm center at time-zero of the 12-km control simulations and the open circle marks the mean position of the storm at time-zero of the 3-km control simulations. The grey region on the 12-km timeline in (b) denotes the 12-hour model adjustment period.

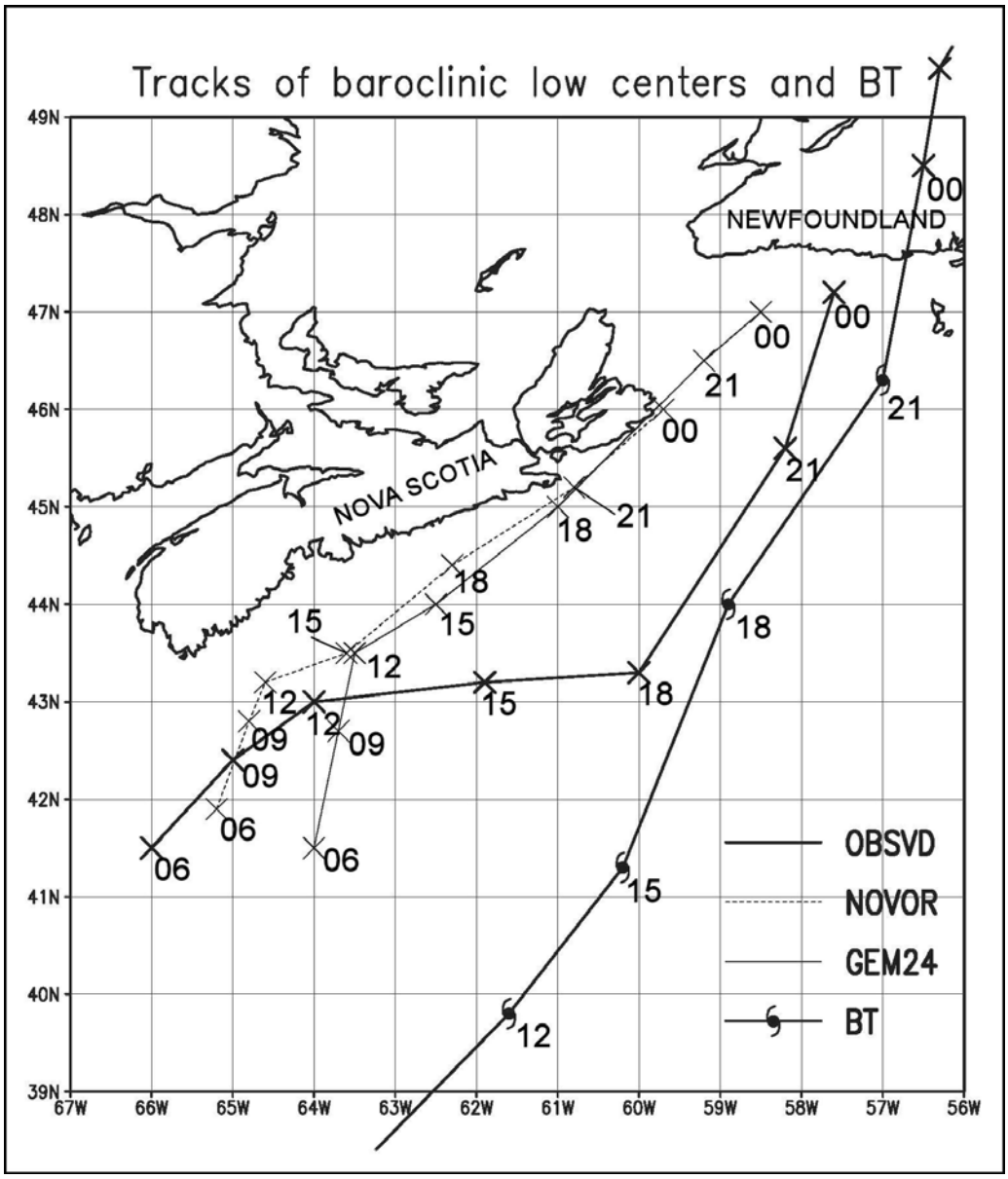

Figure 7. Tracks of the baroclinic cyclone center from observations (OBSVD), the operational GEM model (GEM24), and the no-vortex version of the MC2 model (NOVOR) every three hours from 06 UTC 19 October to 00 UTC 20 October. The best track (BT) segment during the period of interest is also plotted. The valid time for the storm positions in UTC is indicated to the lower right of the position markers.

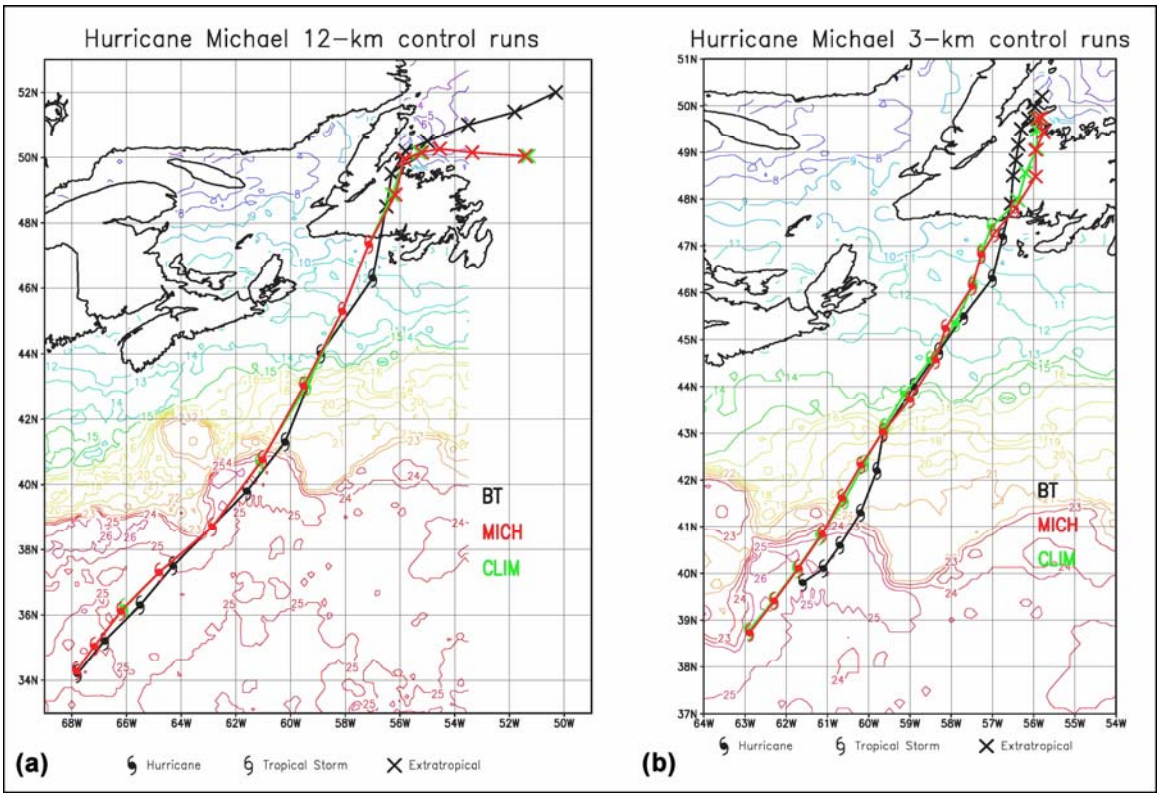

Figure 8. (a) Storm tracks from the 12 km control, and (b) 3 km control runs of the model. Black trajectories denote the "best track", red trajectories denote the observed-SST control run, and green is the climatology SST storm track. Track nodes are every three hours in (a) from 00/19 to 18/20 and every hour in (b) from 12/19 to 06/20. Observed (NESDIS) SST (every 1°C) is also shown.

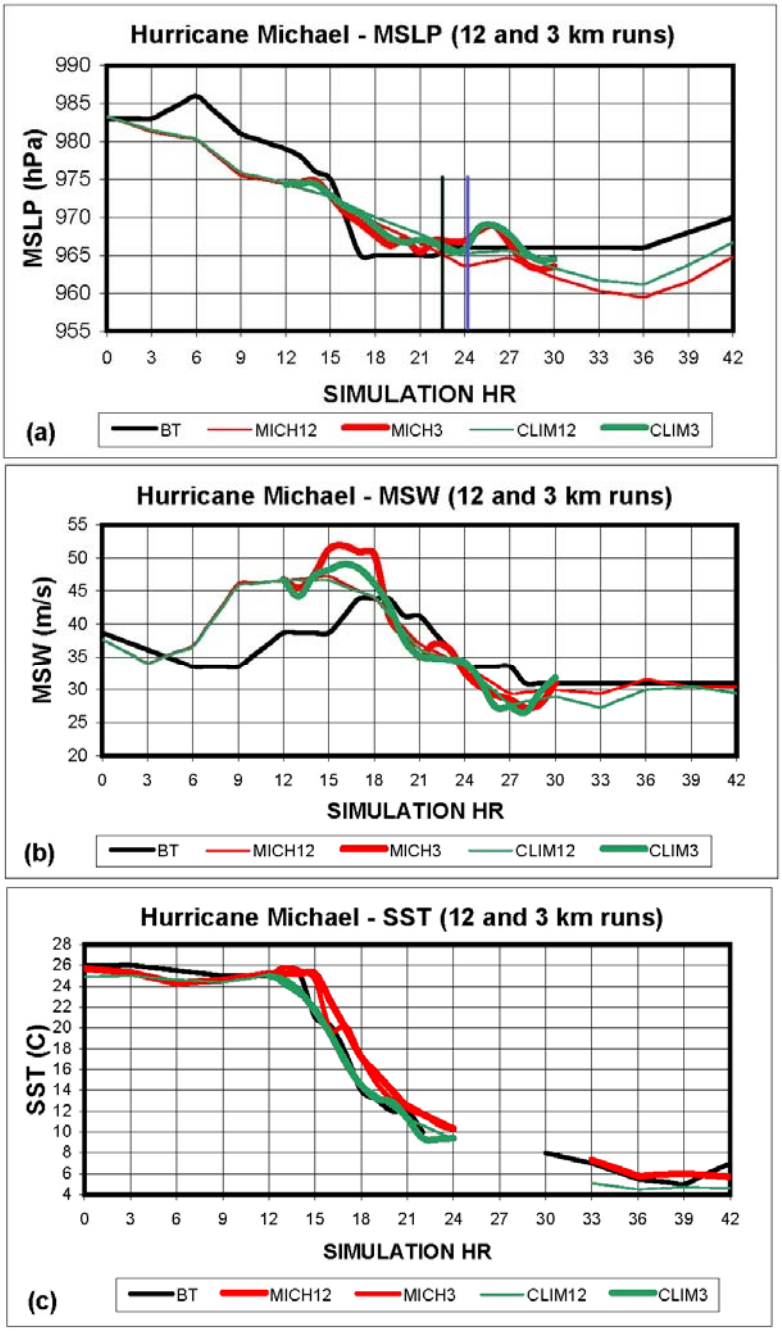

Figure 9. Model results for the 12-km control (MICH12 and CLIM12) and 3-km control (MICH3 and CLIM3) simulations: (a) evolution of minimum sea level pressure (MSLP) for MICH12 (thin red line), CLIM12 (thin green line), MICH3 (thick red line), CLIM3 (thick green line) and the best track (black line); (b) maximum surface winds (MSW); and (c) sea surface temperature (SST) beneath the storm center as a function of model simulation time (hours). The vertical bars in (a) denote the approximate model landfall time (blue) and observed landfall time (black).

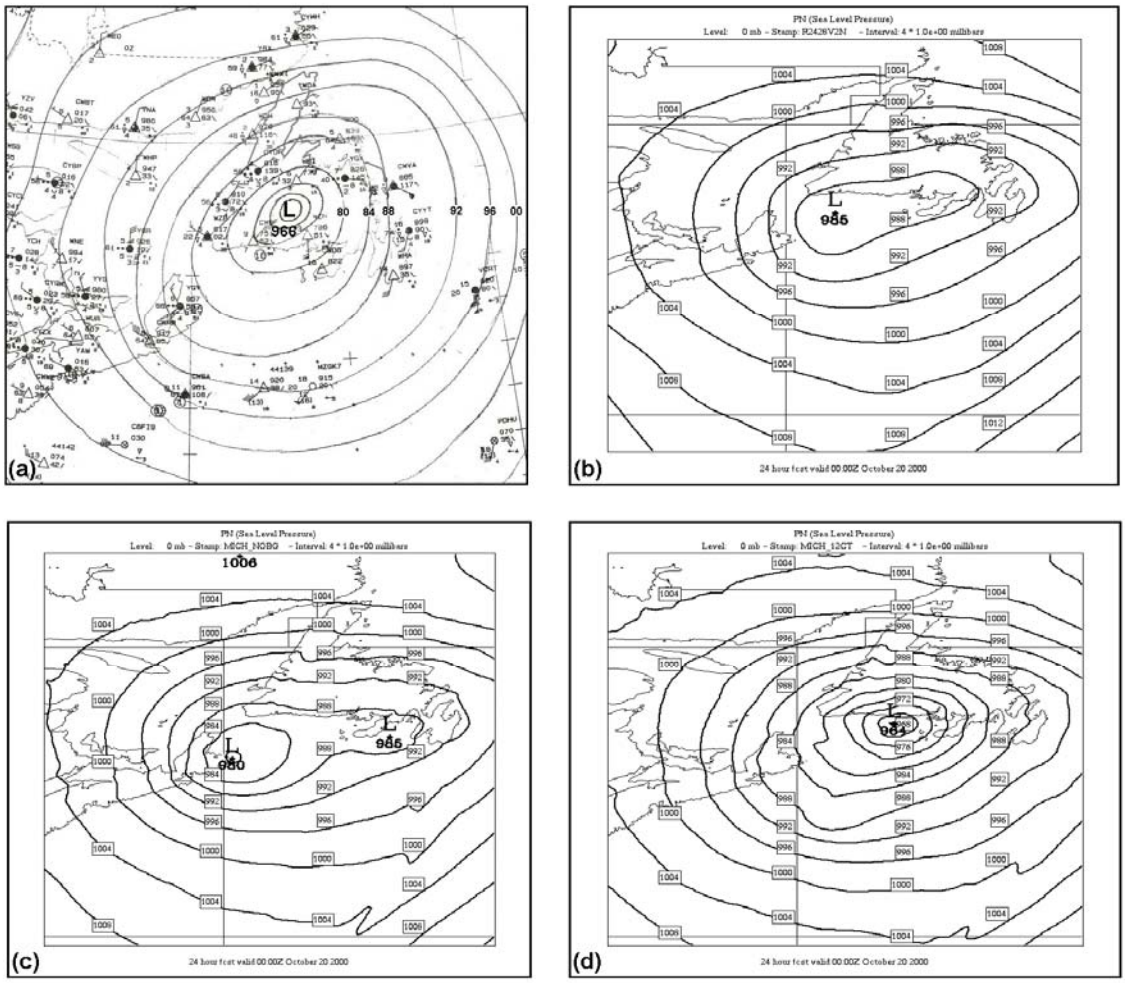

Figure 10. Sea level pressure (every 4 hPa) valid at 00 UTC 20 October based on: (a) manually drawn (subjective) analysis, (b) 24-hour GEM regional forecast, (c) 24-hour "no-vortex" simulation of the 12-km MC2 model, and (d) 24-hour simulation of the control run of the MC2 model with vortex insertion employed (MICH12). Standard synoptic weather plots are shown in (a).

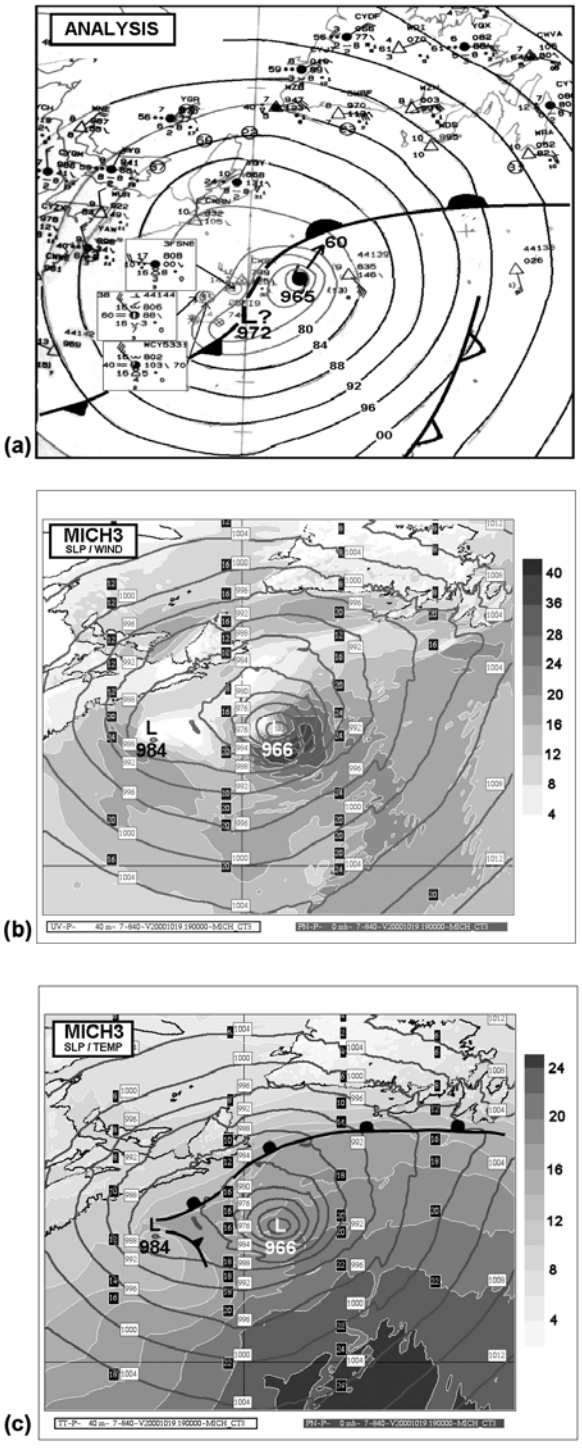

Figure 11. (a) Manually drawn (subjective) sea level pressure (every 4 hPa) valid at 18/19; (b) 3-km model control simulation (MICH3) valid at 19/19 showing sea-level pressure (solid grey contours) and surface (40 m) wind speed (shaded) every 4 m s^{-1}; and (c) same as (b) except with model-simulated surface (40m) temperatures (shaded every 2^{o}C). The estimated position of the baroclinic cyclone in (a) is shown by "L?" and is also marked in (b) and (c).

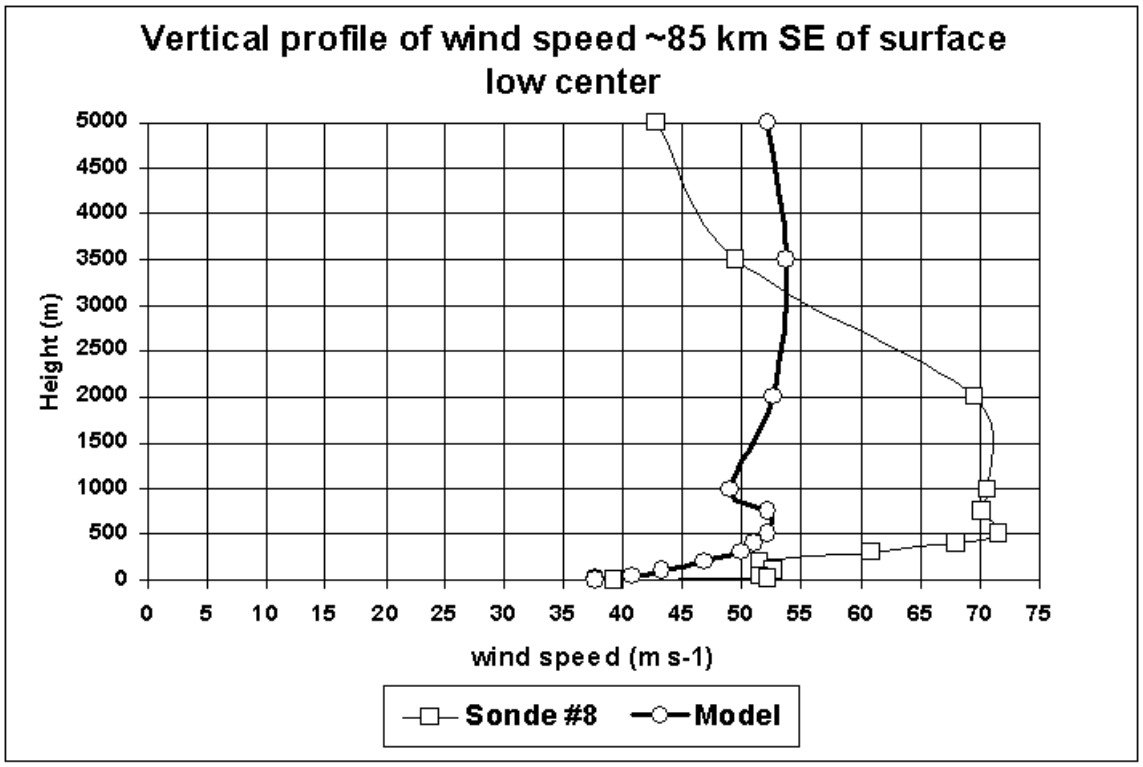

Figure 12. Vertical profiles of horizontal wind speed from aircraft dropsonde #8 at 17/19 and 3-km run of the model (MICH3) at 18/19. The storm-relative position of the profiles is 85 km southeast of the surface position of the hurricane.

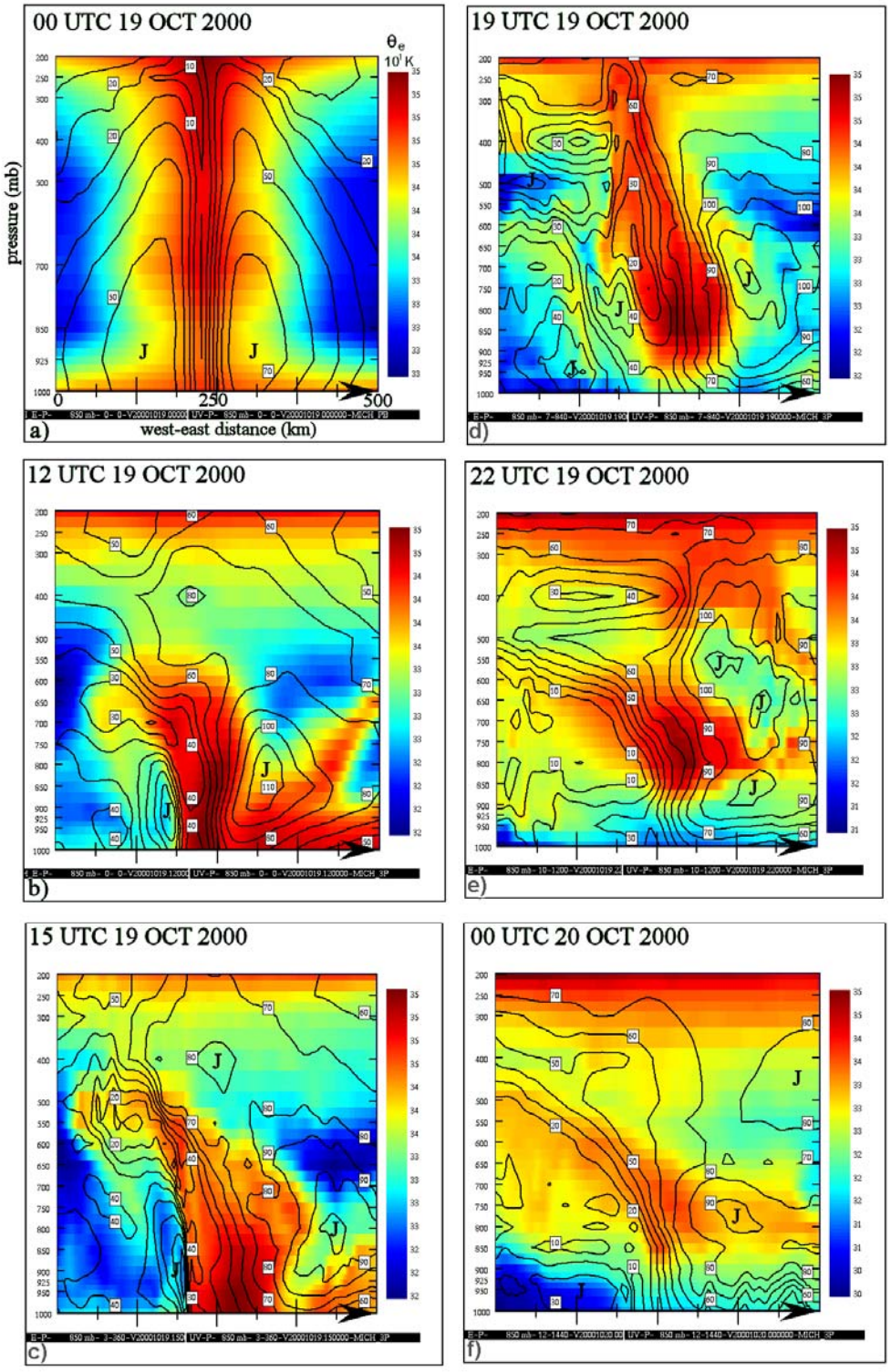

Figure 13. Vertical cross sections of equivalent potential temperature (colored field) and horizontal wind speed magnitude (solid contours every 10 knots – 1 knot = 0.515 m s^{-1}) from the 3-km control simulation (MICH3) at selected times during extratropical transition. The cross sections are taken along a west to east line through the storm center. Panel (a) shows the structure of the synthetic vortex at 00/19.

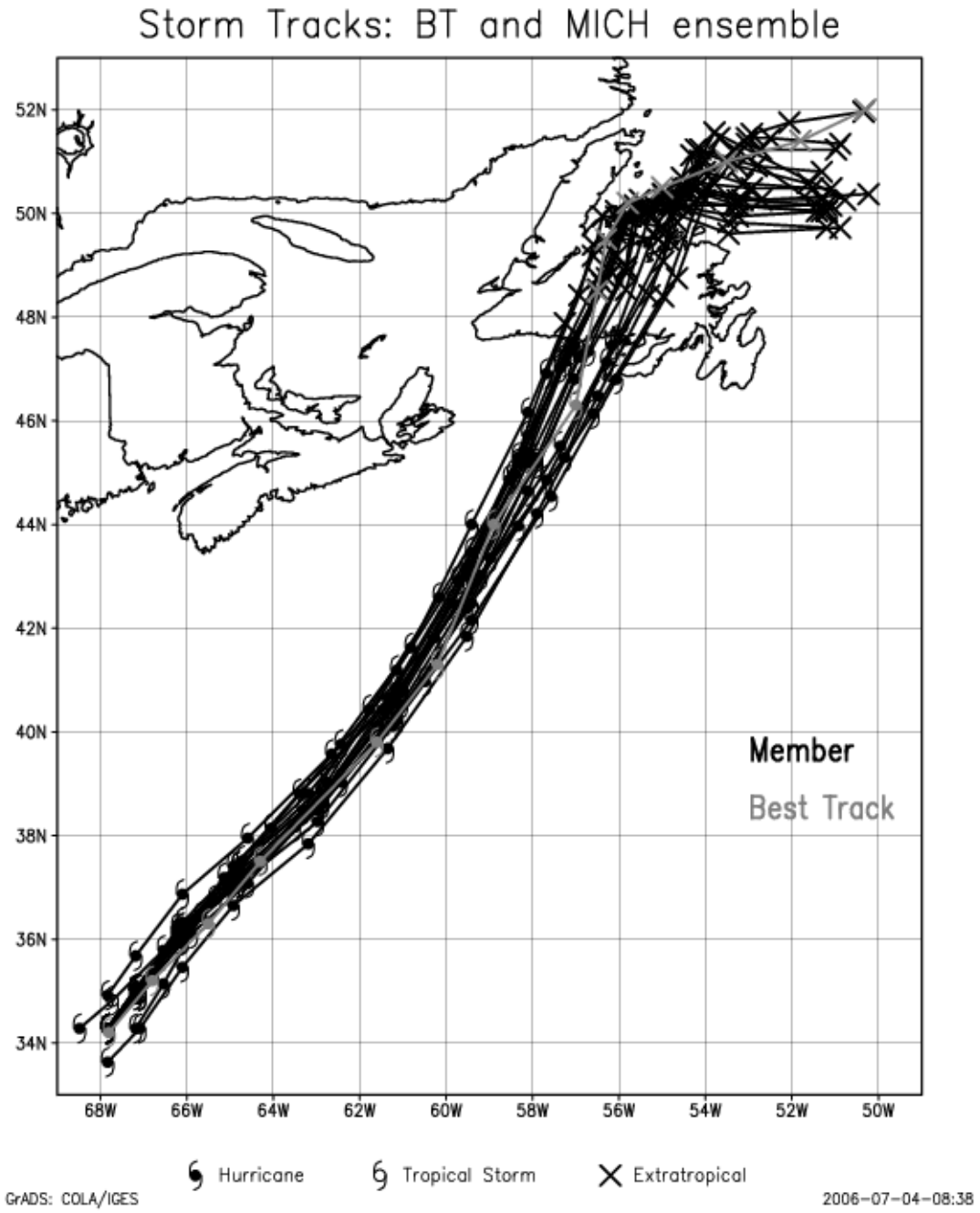

Figure 14. Storm tracks for all ensemble members (including control) from the set of simulations in Table 1 (black), plus the best track (grey). Track positions are every three hours for the 42-hour period from 00/19 to 18/20 October.

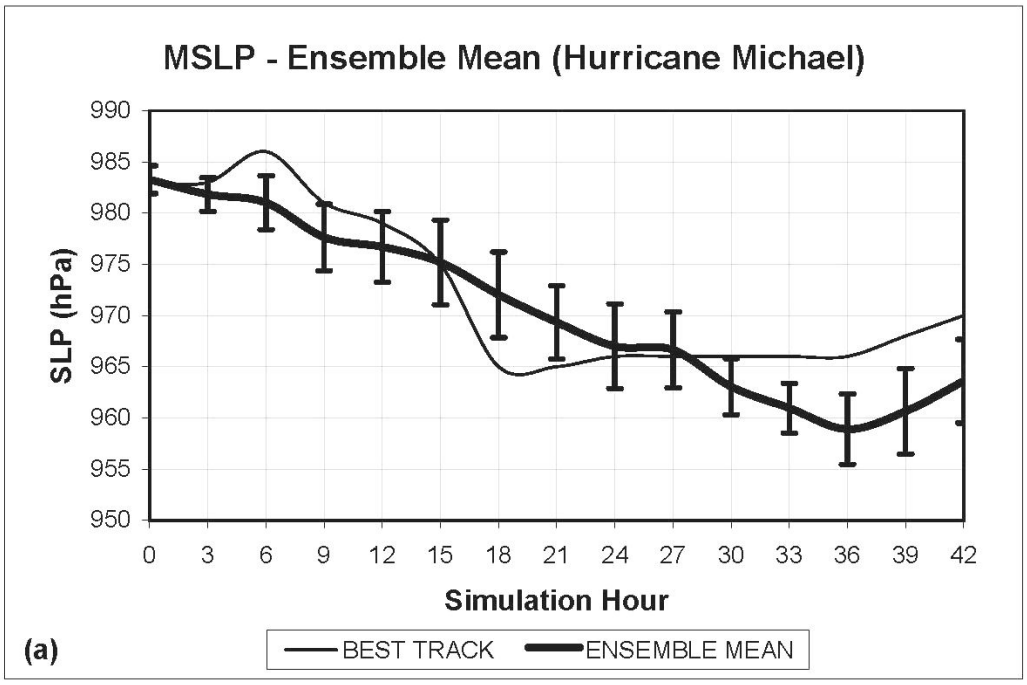

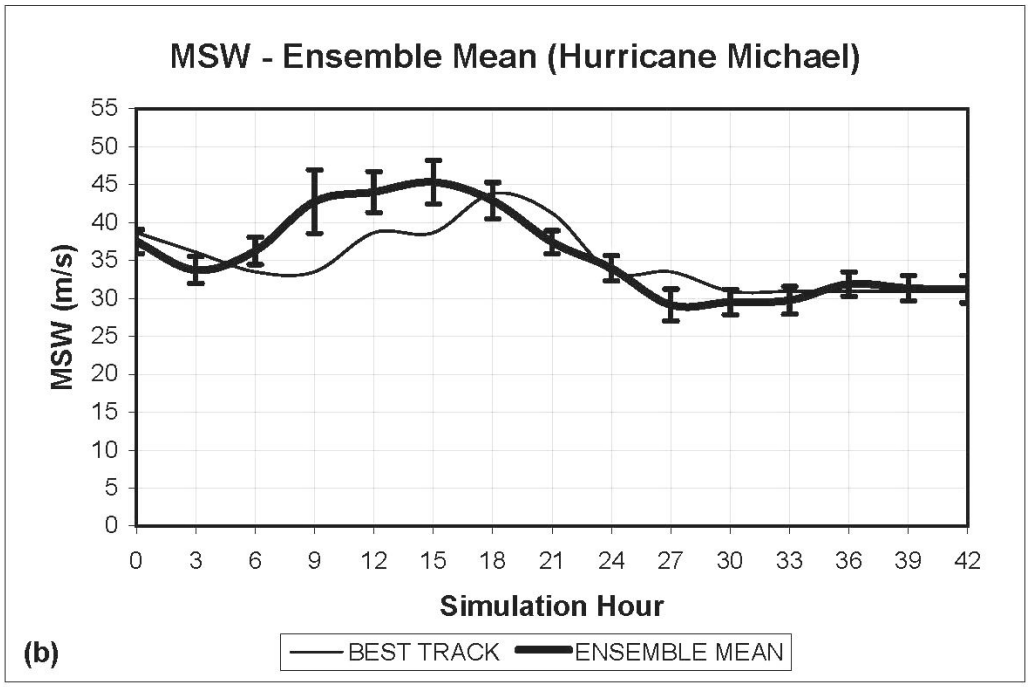

Figure 15. (a) Minimum sea level pressure, and (b) maximum surface wind traces for the ensemble mean (thick curve) and the best track (thin curve). Vertical range bars denote the one-standard deviation values from the ensemble.

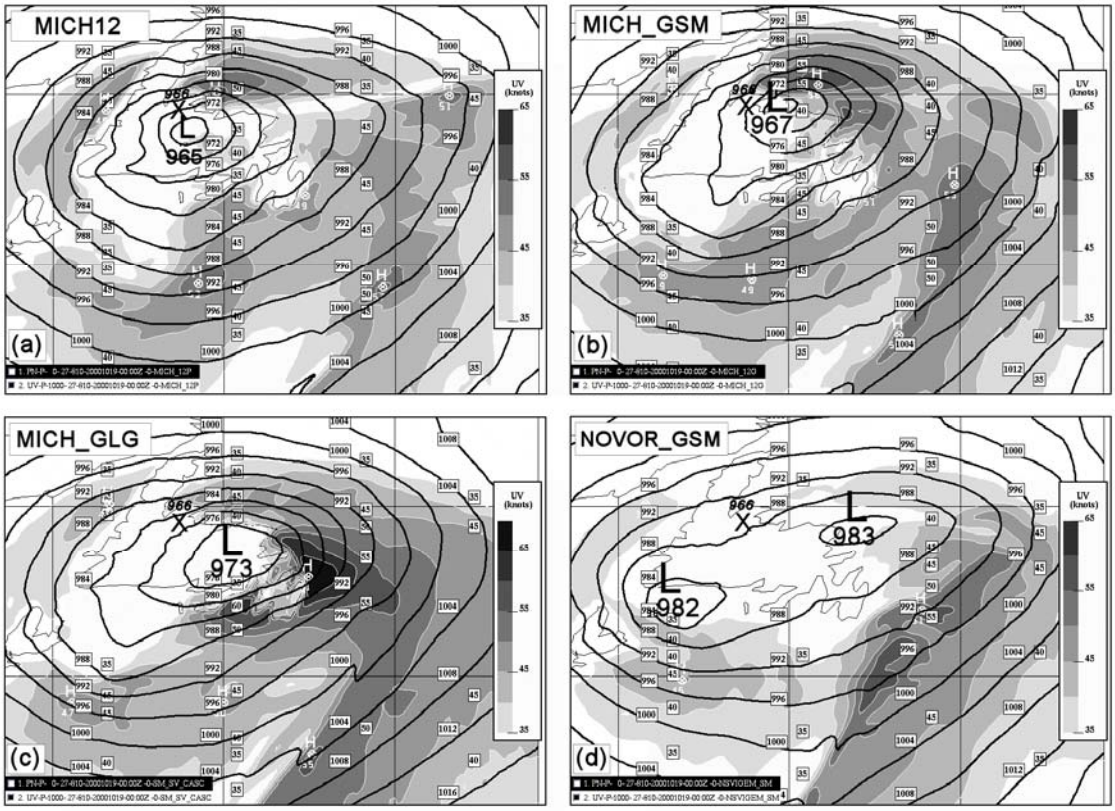

Figure 16. Sea level pressure (black contours) and 1000-hPa wind field (shaded) at simulation hour 27 from the domain and driving-field experiments: (a) small 12 km grid experiment piloted by analyses (MICH12), (b) small 12 km grid experiment piloted by GEM forecasts (MICH_GSM), (c) large 12 km grid experiment piloted by GEM forecasts (MICH_GLG), and (d) small 12 km grid experiment without vortex insertion piloted by GEM forecasts (NOVOR_GSM). Sea level pressure interval is 4 hPa and 1000-hPa wind speed is every 5 kts, where 1 kt = 0.515 m s^{-1}.

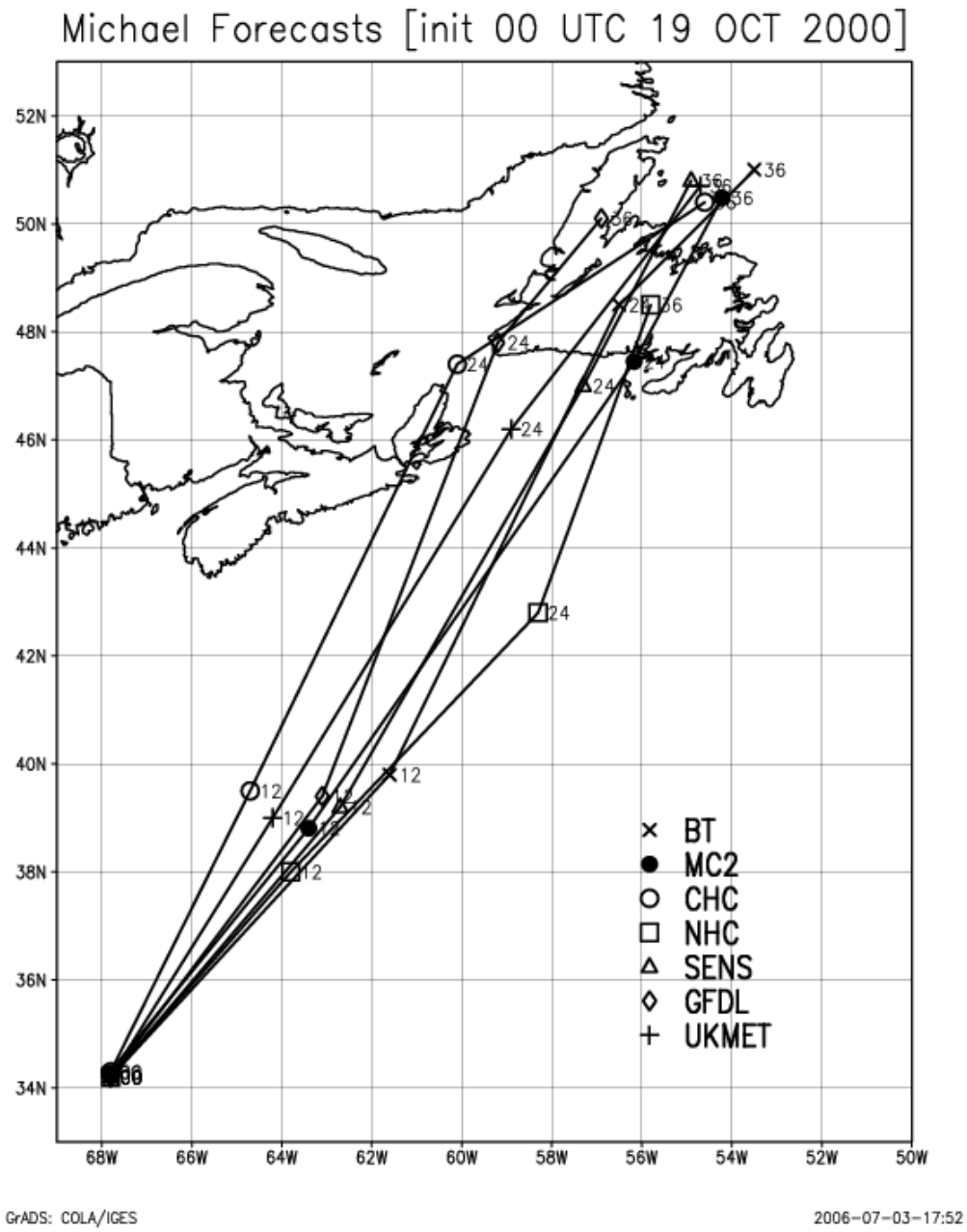

Figure 17. Operational and numerical track forecasts for Hurricane Michael for a 36-hour period beginning 00/19. The acronyms in the legend are defined in the text.

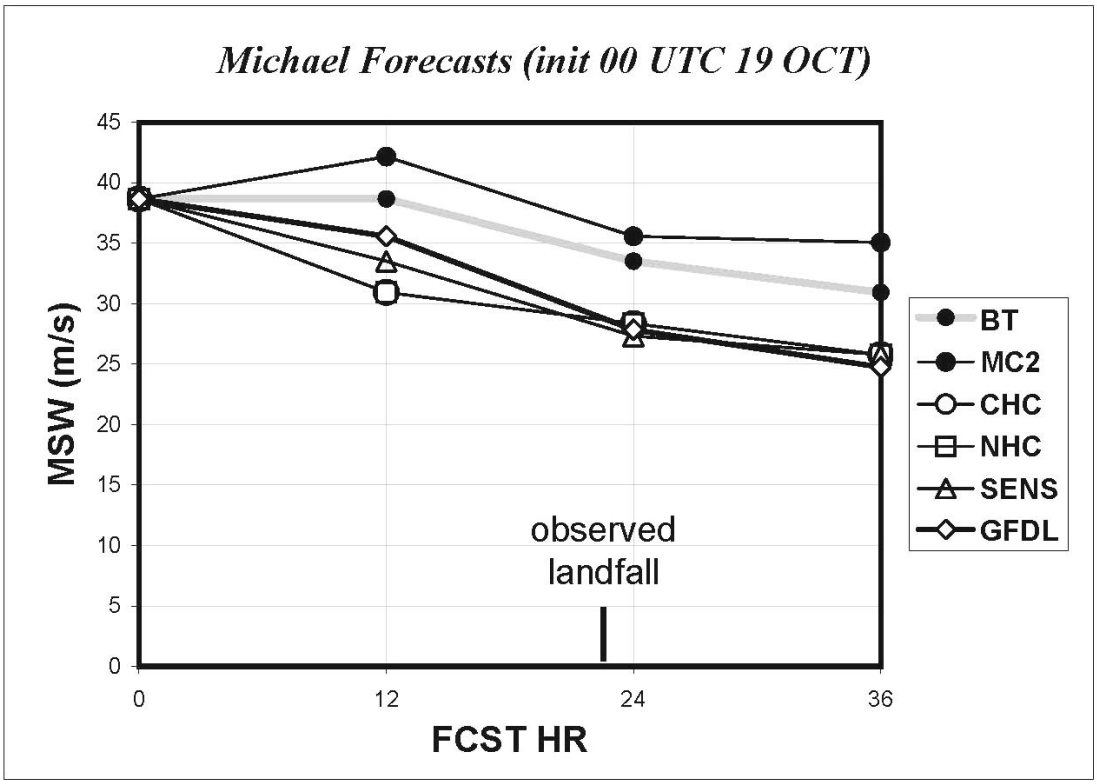

Figure 18. Operational and numerical intensity forecasts in terms of maximum sustained (surface) winds (MSW) for Hurricane Michael for a 36-hour period beginning 00/19. The acronyms in the legend are defined in the text.

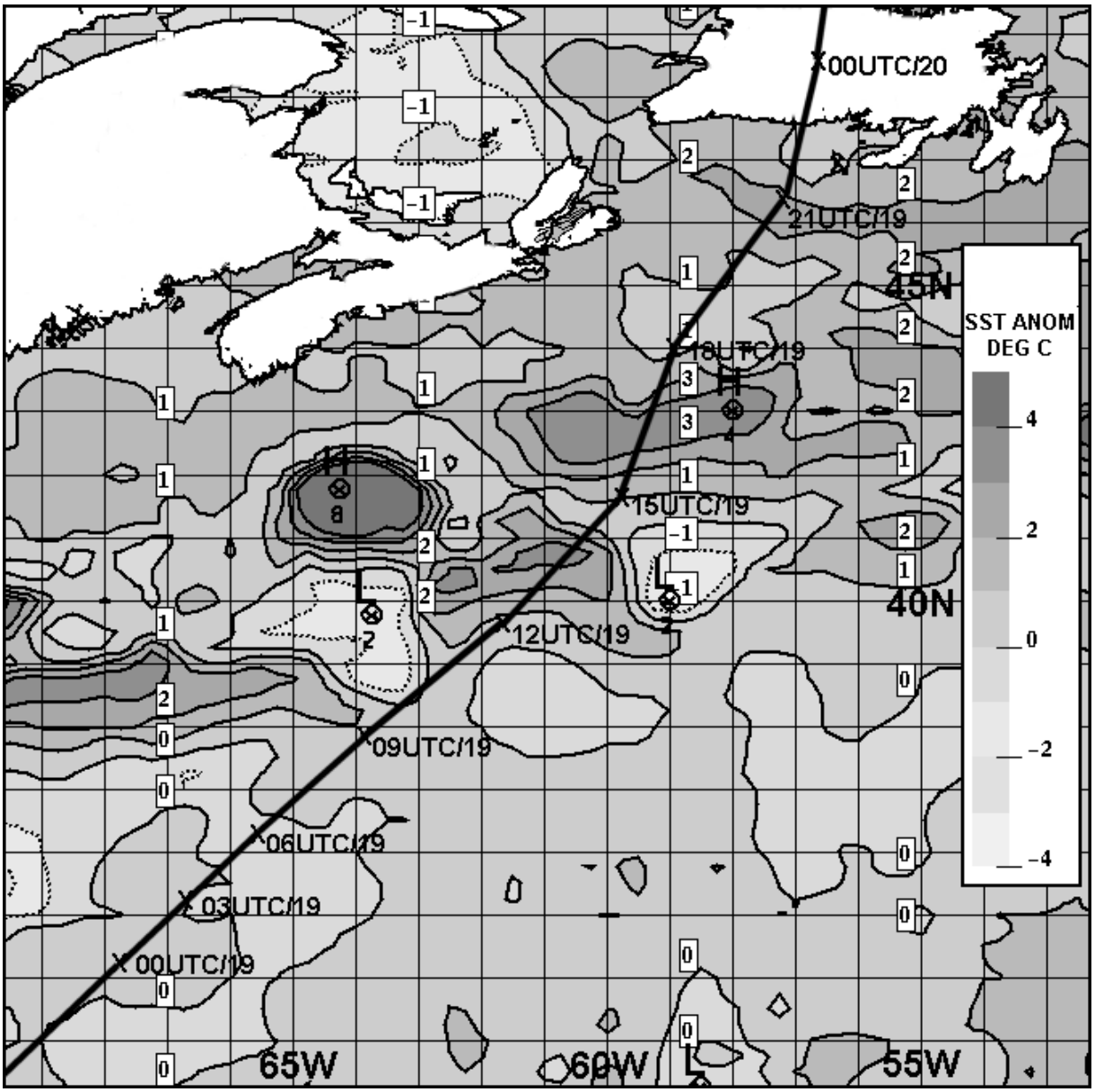

Figure 19. Sea surface temperature anomaly valid at 00 UTC 19 October 2000 (every 1°C). Negative anomaly is represented by dotted contours. Partial storm track for Hurricane Michael also shown.

Experiment	SLP (hPa)	lat (N)	lon (W)	R15 (km)	basicp (frac)	convec	comp_levs ( ) = # in BL	stcond
MICH	983	34.2	67.8	320	0.50	kfc	25(7)	exc
MICH_GSM	983	34.2	67.8	320	0.50	kfc	25(7)	exc
MICH_GLG	983	34.2	67.8	320	0.50	kfc	25(7)	exc
EM1	983	34.2	67.8	320	***0.25***	kfc	25(7)	exc
EM2	983	34.2	67.8	320	***0.75***	kfc	25(7)	exc
ES1	983	34.2	67.8	***290***	0.50	kfc	25(7)	exc
ES2	983	34.2	67.8	***380***	0.50	kfc	25(7)	exc
ES3	983	34.2	67.8	***430***	0.50	kfc	25(7)	exc
EI1	***979***	34.2	67.8	320	0.50	kfc	25(7)	exc
EI2	***987***	34.2	67.8	320	0.50	kfc	25(7)	exc
EP1	983	34.2	***68.4***	320	0.50	kfc	25(7)	exc
EP2	983	***34.9***	67.8	320	0.50	kfc	25(7)	exc
EP3	983	34.2	***67.1***	320	0.50	kfc	25(7)	exc
EP4	983	***33.6***	67.8	320	0.50	kfc	25(7)	exc
EC1	983	34.2	67.8	320	0.50	***fcp***	25(7)	exc
EC2	983	34.2	67.8	320	0.50	***kuo***	25(7)	exc
ER1	983	34.2	67.8	320	0.50	kfc	***32 (10)***	exc
EQ1	983	34.2	67.8	320	0.50	kfc	25(7)	***excrig***

Table 1. List of experiments used in the study with the 12-km grid. MICH12 is the control run using 19 October observed SST surface boundary condition. MICH_GSM and MICH_GLG are the experiments whose lateral boundaries are driven by GEM output fields. Minimum sea level pressure is MSLP, lat/lon indicate the storm center position, R15 is the radius of 15 m s^{-1} winds, "basicp" is the fraction of the background flow used to prescribe the initial wind field asymmetry, "convec" is the convective parameterization scheme, "comp_levs" indicates the number of computational levels in the model, and "stcond" is the stratiform condensation scheme (schemes are explained in the text). Changed parameters in each experiment are in bold italics.